Amylin's role in nociception: study in amylin KO mice

Sara João Lourenço Paulo

Integrated Master in Bioengineering, Molecular Biotechnology

July, 2015

Supervisor

Dr. Catarina Alexandra Soares Potes, IBMC

Co-supervisor

Dr. Fani Lourença Moreira Neto, FMUP

Acknowledgements

I would like to express my sincere gratitude to my supervisor Dr. Catarina Potes, for all the knowledge conveyed, for all the patience, support, availability and friendship. It was an honor to work with such a complete researcher that helped me to grow both professionally and as a person. I will never forget her sympathy, willingness to help and encouragement. I am indeed deeply grateful to her.

Dr. Fani Neto, my co-supervisor, for all support, kindness, availability, encouragement and willingness to help, despite her full professional agenda. Thank you for providing such a nice and healthy work environment.

My colleagues and friends within the research group, it was an honor to work with so pleasant people, always willing to help and so full of joy.

To the Animal Housing of Faculty of Medicine of the University of Porto and animal care takers, for the breeding of the colony used in these experiments and for performing and collecting the ear biopsies necessary for mice genotyping.

To LAIM the Laboratory of Support to Research in Molecular Medicine (LAIMM) at FMUP for performing the DNA extraction and PCR, necessary to genotype the mice.

To whole the Department of Experimental Biology of the Faculty of Medicine of the University of Porto, a sincere appreciation for the warm welcome and constant collaboration.

To my parents, for their unconditional support, for always believing in me and for their wise advice. I wouldn't make it without them. Their absolute love gives me courage and confidence to achieve my goals. I hope they can feel proud of the person I become.

To my sister, for all love, support and encouragement. For all moments we lived together, for making me grow and for never leaving my side. Words fall short in expressing my deep gratitude and admiration.

To my brother-in-law, who supported me all these years. Thank you for your patience and friendship.

My best friend Sara Branco, for all support and sincere friendship which I will never forget. Thank you for being present when I most needed you.

To my friend and colleague Sofia Ferreira, for all support during these extraordinary years. We made it together.

At last, to all my family and friends for unconditional love and support.

Resumo

A dor é definida pela Associação Internacional do Estudo da Dor (IASP) como "uma experiência sensorial e emocional desagradável associada a um dano tecidual real ou potencial ou descrita em termos de tal dano", que pode ter um papel protetor (dor nociceptiva e inflamatória), ou pode ser mal-adaptativa (dor crónica).

A amilina, um membro da família de peptídeos relacionados com o gene da calcitonina, também conhecida como polipeptídeo amilóide, é um péptido com 37 aminoácidos segregado pelas células β-pancreáticas. Esta hormona é segregada simultaneamente com a insulina, em resposta à ingestão de nutrientes. As ações da amilina melhor estudadas a concentrações plasmáticas fisiológicos são na inibição da ingestão de alimentos e do esvaziamento gástrico. Em consequência disso, esta hormona está a ser usada em co-terapia com insulina em pacientes diabéticos nos EUA e é objeto de estudos clínicos de terapias para a redução do peso. O papel da amilina na nocicepção tem sido estudado recentemente, no entanto, as investigações nesta área não são suficientes e os resultados obtidos são muitas vezes contraditórios. Inicialmente foram descritos locais de ligação de amilina em áreas do cérebro envolvidas na nocicepção e a sua presença foi também detetada em gânglios raquidianos dorsais do rato (DRG), sugerindo um papel sensorial deste neuropeptídeo. Após estas descobertas interessantes, alguns grupos focaram-se no estudo do papel da amilina na nocicepção e sugeriram que este péptido pode estar envolvido na fase inicial de inflamação e que pode ter um papel excitatório em condições fisiológicas. Por conseguinte, Gebre Medhin e os seus colegas [2] demonstraram que a depleção genética da amilina produziu um fenótipo em que os ratinhos eram mais tolerantes à estimulação nóxica. Por outro lado, resultados recentes obtidos pelo nosso grupo de investigação mostraram que a administração de amilina em animais com dor inflamatória crónica produziu um efeito analgésico. Além disso, o nosso grupo também observou que a administração de amilina no teste de formalina em rato modulou o comportamento de dor manifestado durante a interfase e a fase de dor sustentada. Os nossos resultados indicam que o efeito da amilina na dor parece variar de acordo com a natureza do estímulo nóxico (aguda/crónica, a origem inflamatória/origem de uma lesão do nervo) e com a via de administração (sistémica/central). Estes resultados sugerem um papel importante de amilina na nocicepção.

O estudo apresentado nesta tese de mestrado teve como objetivo esclarecer o efeito da amilina no sistema nociceptivo por comparação de respostas comportamentais e neuro-químicas entre ratinhos sem o gene da amilina (ratinhos KO) e ratinhos de estirpe selvagem (ratinhos WT). Ambos os grupos de animais foram sujeitos a testes de dor aguda e a três diferentes modelos de dor: dor visceral, dor inflamatória crónica e dor neuropática.

Os testes de dor aguda realizados em ratinhos naïve sugerem que os ratinhos KO são geralmente mais sensíveis aos estímulos mecânicos do que os ratinhos WT. Foram observadas algumas diferenças nos resultados obtidos pelos testes térmicos de dor aguda, uma vez que no teste de Hargreaves não houve diferenças significativas entre os dois grupos de animais, indicando que a falta da amilina em animais KO não causa alterações na sensibilidade ao calor, ao contrário do teste de *Cold plate* em que os animais KO toleraram melhor o frio nóxico do que os animais WT.

A indução de dor inflamatória utilizando o Adjuvante Completo de Freund produziu uma resposta imunitária forte, que resultou numa reação artrítica localizada, resultando no desenvolvimento de uma inflamação grave na pata, de alodínia mecânica e hiperalgesia térmica. Uma vez que as patas ipsilaterais de ratinhos WT apresentaram diferenças significativas em comparação com as patas não inflamadas contralaterais, ao contrário do observado para as patas ipsilaterais de ratinhos KO, pudemos concluir que os ratinhos WT são mais sensíveis aos estímulos nóxicos aplicados.

A indução da dor neuropática foi realizada usando um modelo de lesão parcial do nervo ciático onde dois dos seus três ramos são ligados e axotomizados, denominado SNI (do inglês *spared nerve injury*) e resultou em alodínia e hiperalgesia intensas na região lateral da pata posterior, que recebe inervação do ramo do nervo ciático que foi deixado intacto, a qual se encontra hipersensível. Os resultados observados em testes de dor aguda sugerem que os ratinhos KO foram menos sensíveis aos diferentes estímulos aplicados, mostrando menos sinais de dor neuropática. Estes resultados são suportados pela quantificação de c-Fos, um gene de expressão imediata, que é expresso pelos neurónios rapidamente em resposta a estímulos. Assim, ratinhos WT expressaram mais c-Fos do que ratinhos KO, sugerindo que mais neurónios nociceptivos específicos da medula espinhal foram ativados em ratinhos WT.

A indução da dor visceral foi conseguida através de uma injeção intraperitoneal de ácido acético. As respostas nociceptivas foram medidas através da contagem do número de contrações em intervalos de 5 minutos, durante vinte minutos. Foi observado um efeito temporal e os ratinhos KO contraíram mais vezes o abdómen do que os ratinhos WT no período entre os 5 e os 15 minutos apos injeção, sugerindo um papel anti-nociceptivo da amilina na dor visceral. Estes resultados são suportados pela quantificação de neurónios positivos para o c-Fos na medula espinhal, uma vez que se observou que animais KO expressaram significativamente mais c-Fos do que animais WT.

Para avaliar alterações na densidade neuronal em gânglios raquidianos, foi realizada a coloração por hematoxilina e eosina, sendo o número total de neurónios quantificado. Contudo, não houve diferenças significativas entre os dois grupos

animais. Por outro lado, a medição das áreas neuronais mostrou que os ratinhos KO têm uma tendência para ter mais neurónios de pequeno tamanho (<600 μm^2) e têm significativamente menos neurónios de grande área (>1200 μm^2), em comparação com ratinho WT.

Para avaliar alterações nas populações de nociceptores entre ratinhos WT e KO, os níveis de expressão de CGRP, um marcador bem conhecido de nociceptores do tipo C péptidergicos, foram quantificados. Não foram detetadas diferenças significativas na percentagem de neurónios que expressam CGRP em DRGs da região L4 e L5.

Resumindo, o papel da amilina na nocicepção parece variar dependendo do modelo de dor em causa. Além disso, a falta da amilina em ratinhos KO parece envolver alterações no sistema nociceptivo em populações neuronais especificas dos gânglios raquidianos.

Palavras-chave: amilina, nocicepção, dor visceral, dor inflamatória, dor crónica, alodínia, hiperalgesia, medula espinhal, c-Fos, DRG, CGRP.

Abstract:

Pain is defined by the International Association for the Study of Pain (IASP) as "an unpleasant sensory and emotional experience associated with actual or potential tissue damage, or described in terms of such damage", which may have a protective role (nociceptive and inflammatory pain), or can be maladaptive (chronic pain).

Amylin, a member of the calcitonin gene-related peptide family, also known as islet amyloid polypeptide, is a 37 amino-acid-long secretory product of pancreatic β-cells. This peptide hormone is secreted simultaneously with insulin, in response to nutrient ingestion. The best studied actions of amylin at physiological plasma concentrations are on inhibition of food intake and gastric emptying. Thus, this hormone is being used in co-therapy with insulin in diabetic patients in the US, and is employed in clinical studies for weight reduction. Lately, amylin's role in nociception has been studied, however the investigations in this area are still not sufficient and the results obtained are often contradictory. At first, amylin's binding sites have been described in brain areas involved in nociception and its presence has also been detected in rat's dorsal root ganglions (DRG), suggesting a sensorial role for this neuropeptide. After these interesting findings, some groups focused on amylin's role in nociception and suggested that this peptide could be involved in the initial phase of inflammation and that it could have an excitatory role under physiological conditions. Accordingly, Gebre Medhin and his colleagues [2] have shown that amylin genetic depletion produced a phenotype in which mice are more tolerant to noxious stimulation. On the other hand, recent results obtained by our research group show that chronic subcutaneous amylin administration in animals with chronic inflammatory pain has analgesic effects. Additionally, our group has also observed that amylin administration in the rat formalin test modulates the pain behavior manifested at the interphase and in the sustained pain phase. Our data indicates that amylin's effect on pain seems to fluctuate according to the nature of the noxious stimulus (acute/chronic, inflammatory origin/ origin in a nerve lesion) and to the route of administration (systemic/spinal). Overall, these results suggest an important role of amylin in nociception.

The study presented in this master thesis aimed at clarifying the effect of amylin in the nociceptive system by comparing the behavioral and neurochemical responses of mice with a general ablation of the amylin gene (amylin knock-out, KO, mice) with their wild-type (WT) littermates. Both mice genotypes were subjected to acute pain and to three different models of ongoing pain: visceral pain, chronic inflammatory pain and neuropathic pain.

The acute pain tests performed on naïve mice suggested that amylin KO mice are generally more sensitive to mechanical stimuli than WT mice. Some dissimilarity in

the results were noted when analyzing both thermal acute pain tests, since the Hargreaves test showed no significant differences between both animals groups, indicating no changes in noxious heat sensitivity due to amylin's lack, contrarily to the cold plate test, which suggested that KO animals tolerate better the noxious cold than WT animals.

The induction of inflammatory pain using complete Freund's adjuvant (CFA) elicited a strong immune response that resulted in a localized arthritic reaction, since mice developed a severe paw inflammation, mechanical allodynia and thermal hyperalgesia. As WT ipsilateral hind paws presented significant differences to non-inflamed hind paws, contrarily to what was observed in KO ipsilateral hind paws, we could conclude that WT-CFA inflamed mice were generally more responsive to the noxious stimuli applied.

Induction of neuropathic pain was performed using the spared nerve injury (SNI) model and resulted in long-lasting and intense allodynia and hyperalgesia in the lateral surface of the hind paw receiving innervation from the spared hypersensitive branch of the injured sciatic nerve. The behavior observed in the neuropathic animals in response to acute pain tests suggested that KO mice were less sensitive to the different applied stimuli, showing less signs of neuropathic pain. These results were supported by the quantification of c-Fos immunolabeling, an immediate early gene that is rapidly expressed by neurons in response to stimulation. Thus, WT mice showed more c-Fos positive neurons than KO mice suggesting that more spinal cord nociceptive-responsive neurons were activated in WT SNI-mice.

Induction of visceral pain was done by an intraperitoneal injection of acetic acid. The nociceptive response was measured by counting the number of writhes in 5 minute time-periods for 20 minutes. A time effect was noted and KO animals had in total more writhes than WT animals between 5 and 15 minutes post injection, suggesting an anti-nociceptive role of amylin in visceral pain. These results were supported by quantification of the number of c-Fos positive spinal cord neurons after acetic acid injection, since amylin KO animals expressed significantly more c-Fos than WT animals.

To assess changes on the neuronal density in dorsal root ganglia (DRG), a hematoxylin and eosin staining was performed and the total number of neurons was quantified, but no significant variations were detected when comparing WT and KO animals. However, the measurement of the cell body area showed that KO animals tended to have more small-sized neurons (<600 μm^2) and had significantly lesser amounts of large-sized neurons (>1200 μm^2), comparing to WT animals.

To assess changes in nociceptors populations between KO and WT mice, we also quantified the expression of calcitonin gene-related peptide (CGRP), a known

marker of peptidergic C nociceptors in DRG. We observed no significant differences in the percentage of neurons which expressed CGRP in L4 and L5 DRGs.

Overall, amylin's role in nociception seems to vary depending on the model of pain. Moreover, the lack of amylin in KO mice seems to involve alterations in the nociceptive system in specific populations in the DRG.

Key-words: amylin, nociception, visceral pain, inflammatory pain, chronic pain, allodynia, hyperalgesia, spinal cord, c-Fos, DRG, CGRP.

Index

List of figures

Nomenclature

BDNF	Brain derived neurotrophic factor
CFA	Complete Freund's Adjuvant
CGRP	Calcitonin gene related peptide
CMH	C mechano-heat nociceptors
CNS	Central nervous system
CTR	Calcitonin receptor
DAB	3,3-diaminobenzidine
DRG	Dorsal root ganglia
GABA	γ-aminobutyric acid
H&E	Hematoxylin and eosin
IAPP	islet amyloid polypeptide
IASP	International Association for the Study of Pain
KO	Knock-out
L3-L6	Lumbar 3 until Lumbar 6
L4	Lumbar 4
L5	Lumbar 5
NGF	Nerve growth factor
NHS	Normal horse serum
NS	Nociceptive specific
NSAID	Non steroidal inflammatory drugs
NSS	Normal swine serum
NT-3	Neurotrophin 3
PBS	Phosphate-buffered saline
PBST	Phosphate-buffered saline with triton-X 100
PCR	Polymerase chain reaction
PNS	Peripheral nervous system
PWL	Paw withdrawal latency
RAMP	Receptor activity modifying protein
sCT	Salmon calcitonin
SNI	Spared nerve injury
SNL	Spinal nerve ligation
SP	Substance P
TRPM8	Transient receptor potential melastatin 8
TRPV1	Transient receptor potential vanilloid-1
T5	Thoracic 5
T13	Thoracic 13
T5-L2	Thoracic 5 until Lumbar 2
WDR	Wide dynamic range
WT	Wild-type

Introduction

Nociception

The International Association for the Study of Pain (IASP) defined pain as ''an unpleasant sensory and emotional experience associated with actual or potential tissue damage or described in terms of such damage'' [3]. Pain can be classified as being nociceptive or neuropathic. The first can occur as a result of the noxious stimulation of nociceptors localized on skin, viscera and other organs. When pain is resultant from a dysfunction or lesion in the nervous system, it is classified as neuropathic pain [4]. However, this definition of pain was shown not to be appropriate for animals, as it becomes hard to analyze if an emotional experience occurred or not. Therefore, Zimmermann defined pain as ''an aversive sensorial experience derived from a concrete or potential lesion that causes progressive motor and vegetative reactions, results in behaviors of evasion and can modify specific behaviors of species, including social behavior'' (1986) [5].

Although the pathways of pain perception are not fully described or understood, pain is a process of utmost importance since it is a symptom of many diseases, being considered as a major cause of demand for health professionals among the population in general, as it is very debilitating for the patient. The sensation of pain is present in diseases and in medical procedures and its ineffective treatment can lead to elevated socio-economic costs [4].

Besides the non-steroidal anti-inflammatory drugs (NSAIDs), usually prescribed to alleviate pain of inflammatory origin, the remaining therapies currently used to treat pain are mainly based on the use of narcotic analgesics like morphine, and sedative agents which include barbiturates and benzodiazepines. These agents promote analgesia, i.e., absence or reduction of pain in response to a noxious stimulus. However, these analgesics also produce undesirable side effects, such as depressant actions on respiration [6] and circulation, urinary retention [7], pruritus [7], constipation as well as possible somnolence or drowsiness [8]. Moreover, narcotic analgesics may induce tolerance in patients, as well as dependence.

It is therefore important to invest in the discovery of new more effective therapies that show no significant adverse effects and do not induce tolerance in patients, to combat pain.

From a neurobiological perspective, pain can be classified in three major different types: nociceptive pain, inflammatory pain and, finally, pathological pain, as summarized in Figure 1 [9].

The first one, nociceptive pain, is an early-warning physiological protective system, essential to detect and minimize contact with damaging or noxious stimuli

which can lesion the tissues [9]. This is the pain we feel when touching something too hot, cold, or sharp. This kind of pain is concerned with the sensing of noxious stimuli. It is associated to the stimulus detection and minimizes the contact with damaging stimuli, and so it has a protective role. This protective role demands instantaneous attention and action, which occurs by the withdrawal reflex that it activates, the intrinsic unpleasantness of the sensation caused, and the emotional anguish it involves [9]. Nociceptive pain is, therefore, essential for maintaining the body integrity [9].

Inflammatory pain has also an adaptive and protective role. This pain assists the healing of the injured body part, since it creates a situation that discourages physical contact and movement. The process of inflammatory pain is caused by the activation of the immune system by tissue injury or infection [9]. Pain hypersensitivity, or tenderness, reduces further risk of damage and promotes recovery. In a surgical wound or in an inflamed joint, for example, stimuli that are normally innocuous now elicit pain (allodynia). In this condition, an increased perception of noxious stimuli in the affected area (primary hyperalgesia) or in the adjacent region (secondary hyperalgesia) also occurs [10].

At last, there is pathological pain which is not protective, but maladaptive, and results from abnormal functioning of the nervous system. This pain is not a symptom of disorder but a disease state of the nervous system. It occurs when excessively intense or prolonged stimuli induce tissue damage that results in extended discomfort and abnormal sensitivity. This may arise spontaneously and is characterized by a low threshold to noxious stimuli, causing an exaggerated response to these stimuli, and leading to the presence of primary and secondary hyperalgesia, as well as allodynia. It is caused by tissue damage-associated inflammation (inflammatory pain), or by central or peripheral nerve injury (neuropathic pain) [11].

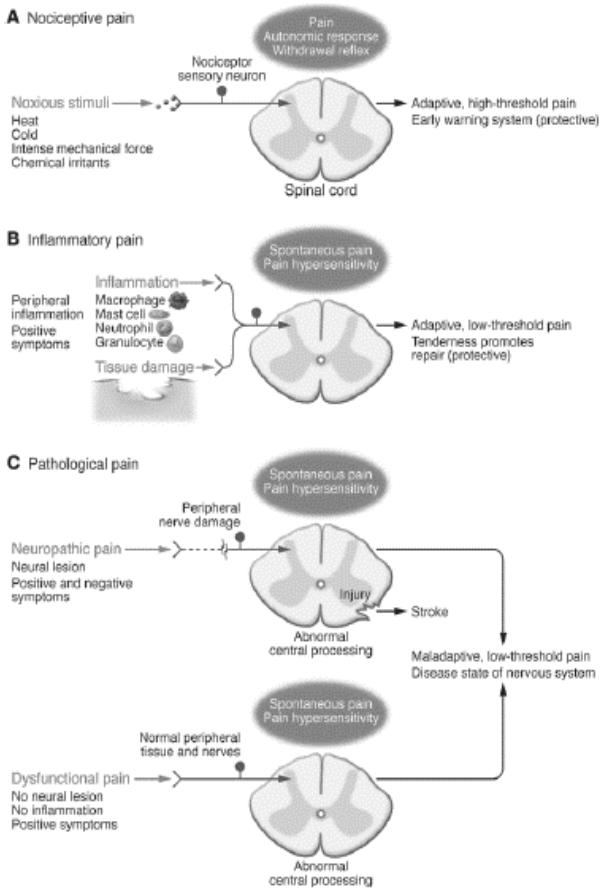

Figure 1 - Pain classification: Nociceptive pain, Inflammatory Pain and Pathological pain. From [9].

Animal Pain Models

Since pain plays an important role on actual society, and its ineffective treatment can lead to elevated socio-economic costs, it has been object of intense research. The major purpose of these studies has been to promote knowledge that will be important to treat acute and chronic pain. To study pain's underlying pathological mechanisms, animal models which mimic different human clinical conditions have been developed throughout the last decades.

Inflammatory Pain Models

In order to understand the mechanisms of persistent pain, animal models of inflammatory pain that simulate human clinical pain conditions have been developed. The majority relies on the injection of inflammatory agents into the rat or mouse hind paw [12]. The main inflammatory agents currently used are carrageenan [13], formalin [14], complete Freund's adjuvant (CFA) and capsaicin [15], although there are more agents available.

Complete Freund's adjuvant injection is a model widely used which consists in the injection of a mycobacteria in a fatty excipient [16] in the animal's hind paw, which will trigger a strong immune response. This method is known for causing pannus formation, cartilage erosion, inflammation and hyperplasia, the same symptoms associated with rheumatoid arthritis, an inflammatory autoimmune disorder [17]. After CFA injection, the cutaneous inflammation appears within two hours and the hyperalgesia and edema are present for at least one or two weeks [17]. It is widely considered as a reliable and useful model to study inflammation and nociception in both rat and mice, which produces a consistent, localized arthritic reaction with associated inflammation-induced nociceptive behavioral changes [18].

Pathological Pain Models: Neuropathic Pain

Neuropathic pain results from trauma in the central (CNS) or peripheral nervous systems (PNS), causing allodynia, hyperalgesia and spontaneous pain. There are several animal models that mimic human peripheral neuropathic pain, which often combine both intact and injured fibers [19]. These models include the spinal nerve ligation (SNL) [20] and the spared nerve injury (SNI) models [19]. The last one consists on the injury of two of the three branches of the sciatic nerve (the tibial and the peroneal nerves) while the third (sural nerve) is left intact. This procedure will induce very rapidly hypersensitivity in the skin area adjacent to the denervation [20].

The SNI has been described as an intense, reproducible and simple model that produces long-lasting and intense allodynia and hyperalgesia for about six months as well as behavioral changes that can be measured by stimulating the non-injured sural nerve skin territory [20]. Acute sensory and pain behavioral tests like the von Frey and Cold Plate, respectively, are conducted to measure hypersensitivity to mechanical and thermal stimuli and the intensity of pain induced in the animals by the axotomy of the tibial and peroneal nerves. Given the similarities to human neuropathic pain and the advantages shown by the SNI model, it is highly used for the study of the mechanisms involved in the development of neuropathic pain and to test the efficacy of new treatments.

Acute Visceral Pain Models

Visceral pain is the most usual form of pain in the clinical setting and one of the most relevant reasons for patients to seek medical supervision [21]. It results from pain in the internal organs and is described as being vague, poorly defined and more similar to a discomfort than a real sense of pain. Visceral pain is usually perceived indistinctly in the same site (lower sternal region of epigastrium) no matter what organ is involved [22].

In order to induce this type of pain in rats or mice, it is usual to perform an intraperitoneal injection of a noxious agent [22]. This method is called ''the writhing

test''. After the injection of the chemical irritant, the animal will respond with characteristic contractions of the abdominal muscles accompanied by a hind limb extensor motion. The most frequently used agents for the writhing test have been phenylquinone and acetic acid [23].

Intraperitoneal injection of acetic acid is a well-known noxious chemical visceral stimulus in animals that produces the already mentioned abdominal contractions or writhes, and also affects the gastrointestinal ileus by inhibiting gastric emptying and small intestine transit, which is associated with visceral pain [24].

Nociceptors

The PNS neurons responsible for the detection and transmission of noxious stimuli are known as nociceptors [25]. The nociceptor has four major functional components: the peripheral terminal that transduces external stimuli and initiates action potentials, the axon that conducts action potentials, the cell body that controls the identity and integrity of the neuron and is localized in sensory ganglia, and the central terminal which forms the presynaptic element of the first synapse in the sensory pathway in the CNS (Figure 2) [26]. Stimuli arising from the face and head will be sensed by nociceptors with their cell bodies located in trigeminal sensory ganglia while stimuli in the remaining parts of the body will be conducted to cell bodies located in dorsal root ganglia (DRG).

Figure 2 - Schematic drawing of nociceptor's structure. It is represented the location of the cell body of a nociceptor responsible for detecting stimuli in all parts of the body except the face and head. From: [25]

Each nociceptor structure has an essential role in the perception and transduction of the stimulus. The cell body is necessary to maintain the other regions of the cell and is located in the ganglia of the spinal cord dorsal roots, as already mentioned. The axon detects peripheral stimuli, transduces their energy into an electrical signal and conducts the action potential to the synaptic terminal where the information is transmitted to the primary sensory area. Thus, stimuli arising from trigeminal ganglia will be conveyed into the trigeminal nucleus while stimuli from DRG, arising from any part of the body except the face and head, will convey into the dorsal horn of the spinal cord. These stimuli can be thermal, mechanical or chemical from

different parts of the organism. The release of transmitters at the synaptic terminal is subject to modulation by agents released by other neurons and possibly by glial cells [25].

Nociceptors can be broadly divided into two classes: one class has small-diameter cell bodies and slowly conducting, unmyelinated axons (C fibers), whereas the other class has medium-diameter cell bodies and faster conducting, lightly myelinated axons (Aδ fibers) [27]. There are also Aβ fibers which transmit non-nociceptive information [4]. These different fibers are divided into three big groups, in result of their different conduction velocities, fiber diameter and myelination, as it is shown in Table 1:

Table 1 - Classification of cutaneous sensitive fibers

Fiber	*Myelination*	*Conduction velocity*	*Fiber Diameter*
Aβ	Thick	30-100 m/s	>10 µm
Aδ	Thin	12-30 m/s	2-6 µm
C	Absent	0,5-2 m/s	0,4-1,2 µm

Nociceptors can also be further divided into three groups according to their neurochemistry: peptidergic C nociceptors, non peptidergic C nociceptors and Aδ nociceptors. All of them have glutamate, the most abundant excitatory neuropeptide. However, the peptidergic C nociceptors also express substance P (SP) and the calcitonin gene related peptide (CGRP). These CGRP-containing neurons are activated by chemical, thermal, and high-threshold mechanical stimuli, and innervate essentially all peripheral tissues [28]. They also send primary afferent input to nociceptive and viscerosensitive neurons in the dorsal horn, trigeminal nucleus caudalis, or nucleus of the solitary tract that project to the brainstem, amygdala, hypothalamus, and thalamic nuclei, which in turn transmit these inputs to the somatosensory and insular cortexes [28]. This group of nociceptors relies on neuronal growth factor (NGF) for developing and survival.

The second group of nociceptors (non peptidergic C nociceptors) does not have peptides and depends on brain derived neurotrophic factor (BDNF) for their development and survival. This later type of nociceptors can be identified for the presence of specific isolectins, purinergic receptors or other specific enzymes. The final group, Aδ nociceptors, relies on neurotrophin-3 (NT-3) and BDNF and is easily recognized by the presence of specific neurofilaments [4].

Responses to stimulus

As mentioned above, Aβ fibers are responsible for sensing innocuous stimulus, like vibration and pressure. Under physiological conditions, C and Aδ fibers conduct nociceptive information [4]. When a noxious stimulus is applied, Aδ fibers are responsible for the immediate acute pain, exhibiting a high conduction velocity of the stimulus. On the other hand, C fibers are responsible for a more diffuse delayed pain sensation, as these fibers exhibit a lower conduction velocity and diameter [4].

Aδ fibers can be divided into type I and type II Aδ fibers [4]. Type I fibers respond mostly to mechanical stimulus, but can also respond to chemical and thermal stimulus above 53^{o}C [29]. Type II Aδ fibers are insensible to mechanical stimuli, but respond to lower thermal stimuli than Aδ fibers type I.

C fibers can be divided according to the noxious stimulus that activates them. Many of them are polymodal, so they respond to all different stimuli (mechanical, thermal and chemical) [27]. However, some C-nociceptors are only sensitive to thermal or mechanical stimulus, or to both [4].

The C fibers which are simultaneously sensitive to mechanical and thermal stimuli are known as C mechano-heat nociceptors (CMH) and are activated by a range of pressures from 30 to 17 mN in human and mice and by temperatures around 39-51^{o}C [30]. Moreover, there are other types of C nociceptors that are insensitive to noxious mechanical and heat stimuli, known as silent nociceptors. These nociceptors are present in skin, viscera and joints. In case of inflammation, where there is release of histamine or other substances, these C silent nociceptors are capable of being activated by noxious stimuli, exhibiting a decrease in their activation threshold [31].

Central projections of nociceptors

The spinal cord consists of a gray inner zone covered by white matter. This gray zone is divided in ten laminae, which are anatomically and electrophysiological distinct [32]. The lamina I (or marginal zone) is the more superficial region of the dorsal horn, which extends to lamina VI. The ventral horn comprises laminae VII-IX and the center canal is surrounded by lamina X (Figure 3).

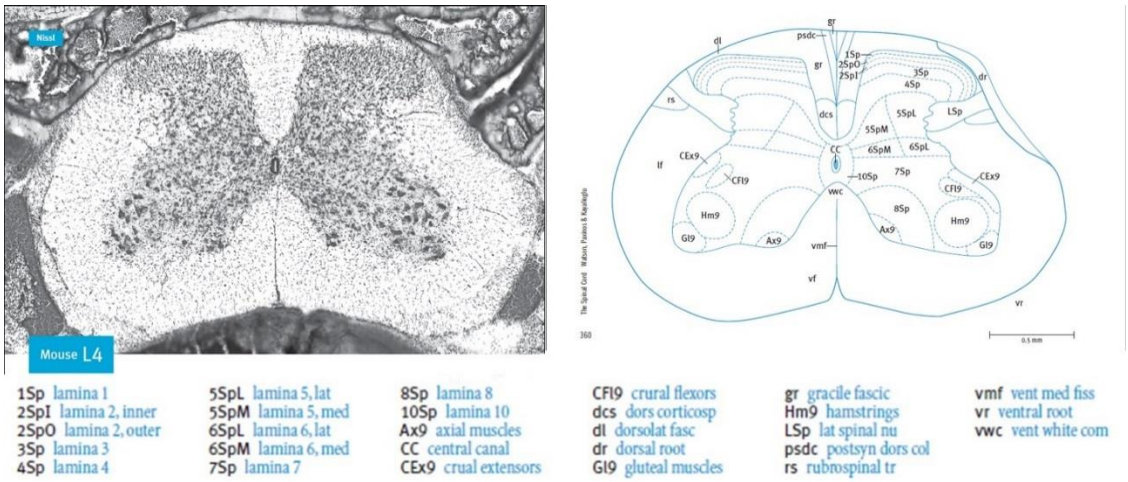

Figure 3 - Illustration of a lumbar 4 (L4) cross section of the mouse spinal cord. Left: Nissl staining of a L4 cross section of the mouse spinal cord. Right: respective atlas schematic drawing from [33].

The central projections of the different types of nociceptor are distributed differentially in the spinal cord, occupying different areas and, therefore, different laminae [32]. Aβ nociceptors, responsible for transmitting innocuous information, terminate in laminae III and IV. They also terminate in lamina V, as well as Aδ and C fibers, where convergent non-noxious and noxious inputs are received [32]. Most peptidergic C fibers terminate in lamina I and in the most dorsal part of lamina II. On the other hand, the non-peptidergic afferents terminate in the mid-region of lamina II. Electrophysiological analyses demonstrate that spinal cord neurons within lamina I are generally responsive to noxious stimulation (via Aδ and C fibers) (Figure 4).

Spinal cord neurons can be divided in three major groups, considering their functional features. They can be nociceptive specific (NS) therefore responding to noxious stimuli only; non-nociceptive, which respond equally to both innocuous and noxious stimuli, and wide dynamic range (WDR) neurons, which respond to both noxious and innocuous stimuli according to their intensities, so that the response is proportional to the intensity of the stimulus [32].

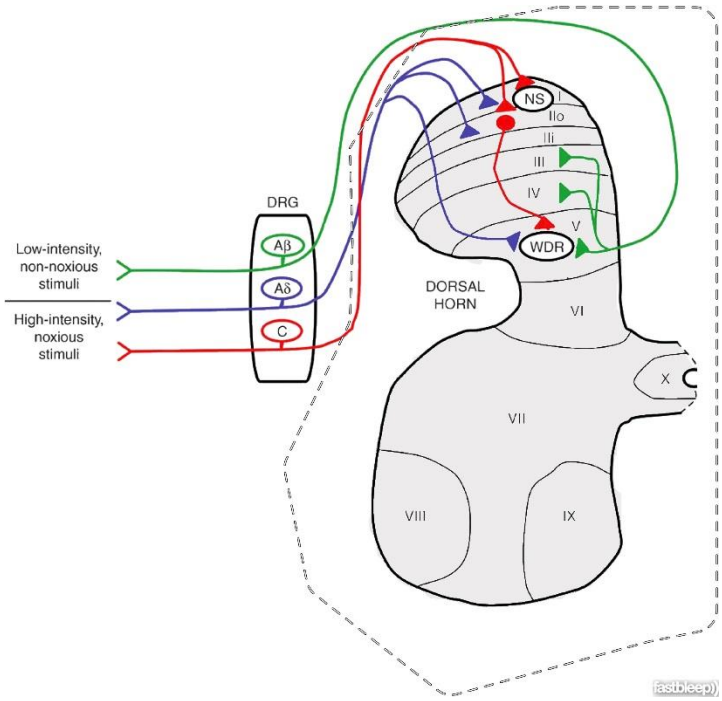

Figure 4 Spinal cord anatomy. NS: nociceptive specific neurons; WDR: Wild-dynamic range neurons. Adapted from: [34]

Neurons in the spinal cord can also be classified as being inhibitory or excitatory, or according to the terminus of the axon relatively to the cell body as interneurons, propriospinal or projection neurons. Interneurons communicate with nearby neurons, propriospinal neurons connect with other regions of the spinal cord, in particular the contralateral side, and projection neurons, which are mainly present in laminas I, V and X, have long axons and transmit the information from the spinal cord to supraspinal regions such as the thalamus and parabrachial area. The thalamus activates the pain matrix while the parabrachial area is involved in descending and affective modulation [35], facilitating or inhibiting the transmission of painful information from the spinal cord.

During nociceptive transmission, the output of the spinal cord is dependent on various spinal mechanisms that can increase or decrease the activity of dorsal horn neurons. These mechanisms comprise local excitatory and inhibitory interneurons [34]. The inhibitory neurons release γ-aminobutyric acid (GABA) and/or glycine, while the preferred neurotransmitter for the excitatory neurons is glutamate.

Neuronal markers

The study of the expression of some neuronal markers can be very useful to determine the amount of noxious information that is being transmitted to the CNS by primary afferent neurons.

Quantification of c-Fos expression has been widely used as a marker of neuronal excitation [36] and is easily detected by an immunohistochemistry reaction.

The immediate early gene c-Fos is quickly expressed by spinal cord neurons following noxious stimulation of the body tissues and its laminar distribution is connected to the nature of the sensory stimulus [37]. Its transcriptional activation takes place within minutes after noxious stimulation and the levels of this proteins reach its peak about two hours after stimulation [38] and returns to baseline values after eight to twenty-four hours after the initial stimulation [39]. It is widely accepted that analysis of c-Fos expression may help clarify the central neural activity occurring during the development of persistent pain or prolonged inflammatory pain [40]. Indeed, in the spinal cord, c-Fos expression is considered specific of neurons activated by noxious stimulus while its supraspinal expression may occur independently of a painful stimulus [35].

Another cellular marker related to the nociceptive system is the calcitonin gene related peptide (CGRP). CGRP is a 37–amino acid peptide that is a member of the calcitonin family and is widely expressed in the PNS and CNS, frequently coexisting and interacting with other neurotransmitters [28]. CGRP is known for its vasodilator properties and for participating in many central and peripheral pain mechanisms. It is upregulated in peripheral nerve injury or tissue inflammation conditions and produces sensitization of dorsal horn and trigeminal neurons. CGRP is also known for eliciting behavioral pain sensitization [28]. Thus, CGRP is considered a classic marker of nociceptive DRG neurons [41], namely, C-peptidergic nociceptors as mentioned above, which respond to stimuli that evoke sensations of pain and itch. As for c-Fos, its expression is easily detected by an immunohistochemistry reaction.

Amylin

Amylin, also known as islet amyloid polypeptide, is a 37 amino-acid-long beta-cell secretory product and the main protein component of the pancreatic islet amyloid found in human subjects with type 2 diabetes (Figure 3). Amylin is a product of a gene located on chromosome 12. It is transcribed as an 89-aminoacid prepolypeptide, is cleaved to form the mature peptide in the β-cells of the pancreas, where it is stored along with insulin and C-peptide in the same granules. Amylin is a normal product of β-cells and is co-released with insulin in a molar ratio of 1 to 100 in healthy non-diabetic subjects in response to nutrient stimuli (carbohydrate-and protein-containing meals) [42] although this rate is not always constant.

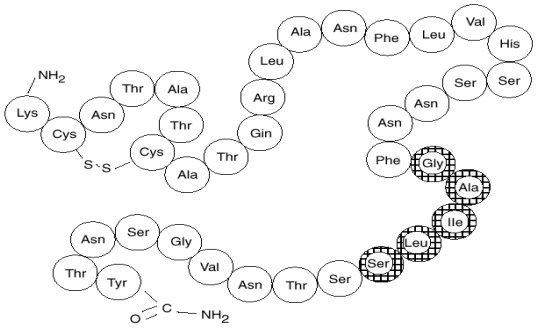

Figure 5 - Amino acid sequence of human amilyn. [43]

Effects of amylin

Some of amylin's physiological functions include decrease of appetite [44], inhibition of gastric emptying, gastric acid and of secretion of digestive hormones [45], therefore amylin controls nutrient appearance in plasma, and plays an important role in weight control.

Amylin presents a regulatory effect on glucose homeostasis, presenting an important role on the control of insulin secretion, as it was reported that amylin inhibits insulin secretion [46]. While the human amylin peptide readily forms aggregates, as mentioned above, rat amylin does not. Therefore, co-therapy treatments in type 2 diabetes mellitus patients use a soluble and stable rat amylin analogue (pramlintide) to control glycaemia in these patients [47]. Additionally to these roles of amylin there are reports of other functions, many of which totally unrelated to metabolism control, such as induction of kidney's epithelial cells proliferation [48], development of proximal tubules [49], differentiation of osteoclasts and osteoblasts, protection of the gastric mucosa [50], blood pressure regulation where it functions as a vasodilator [51], modulation of memory [52] and of motor activity [53].

Calcitonin and Calcitonin Gene Related Peptide (CGRP)

It is known that some actions of amylin are identical to the known metabolic actions of CGRP and calcitonin. In fact, these peptides belong to the same peptide family and possess related structures.

Amylin's structure is 50% identical to that of CGRPs, 37 amino acid peptides which are widespread neurotransmitters with many potent biological actions [51]. CGRP is formed from the precalcitonin gene on chromosome 11 [54] and as result of transcription, two different peptides are produced by alternative splicing: procalcitonin (in thyroid tissue) and proCGRP (in neural tissue).

Calcitonin is a 32 amino acid peptide which is produced by thyroid C-cells. Calcitonin is synthesized at first as a 132 amino acid precursor molecule and then is processed by proteolytic cleavage and by amidation of its carboxy terminal proline residue before secretion [55].

The gene which encodes calcitonin is also responsible for encoding one of the CGRPs, the α-CGRP, which is largely expressed in neural tissue, in both PNS and CNS. α-CGRP is known to be a potent vasodilator [55]. Cell specific alternate processing of the calcitonin/α-CGRP transcripts is the mechanism that regulates the formation of either calcitonin or α-CGRP in different cell types.

Another molecule described as being very similar to calcitonin and α-CGRP is β-CGRP. This is a product of another gene which is expressed by enteric neurons and it differs from α-CGRP by just 3 amino acids in humans [55].

The peptides just described are extensively distributed in various peripheral tissues as well as in the PNS and CNS and induce multiple biological effects. Effects such as vasodilatation (CGRP) and inhibition of bone resorption (calcitonin) are shared, though with much less potency, by amylin [56].

Amylin's receptor

Earlier reports suggested that amylin acted via CGRP receptors in order to achieve its biological effects. Later it was discovered that amylin receptors can be reconstituted in cellular systems by co-expressing the calcitonin receptor (CTR) with receptor activity modifying proteins (RAMPs). These receptors exhibit high affinity for salmon calcitonin, which is recognized as a very potent agonist of amylin receptors, while, importantly, CGRP shows much less affinity for these receptors [56].

The specific amylin receptor is a heterodimeric complex that consists on the association of CTR with one of the three RAMPs, RAMP1, RAMP2 or RAMP3 (Figure 4) [57], having high affinity for amylin [58]. It is known that the CTR belongs to the family of the G protein-coupled receptors which have 7 transmembrane domains. Analysis of CTR transcripts from the porcine kidney epithelial cell line LLC-PK_1 has exhibited two splice variants, CTR1a and CTR1b, being this last transcript longer due to the presence of an additional 48 base pairs coding sequence [59]. These receptors induce the accumulation of cyclic AMP, leading to activation of the subordinate signaling cascade. As previously stated, RAMPs play an important role in this receptor's structure, offering a mechanism for the ligand specificity variation and regulation of receptor function. These proteins have the ability to enhance the affinity of CTR to amylin, building up the amylin receptor. When associated with a calcitonin like receptor, RAMPs build up the CGRP receptors.

Six different isoforms of amylin receptors were reported: $AMY_{1(a)}$ (CTRa/RAMP1), $AMY_{2(a)}$ (CTRa/RAMP2), $AMY_{3(a)}$ (CTRa/RAMP3), $AMY_{1(b)}$ (CTRb/RAMP1), $AMY_{2(b)}$ (CTRb/RAMP2) and $AMY_{3(b)}$ (CTRb/RAMP3), being the most common ones $AMY_{1(a)}$ and $AMY_{3(a)}$. CTR(b) displays greater capacity to generate RAMP2 AMY receptors than CTR(a) [56]. It was also reported that different RAMPs promote different pharmacologic properties and different affinities for the ligands. For

example, RAMP3 provides a greater affinity for salmon's calcitonin and amylin while RAMP1 increases CTR affinity for mammal's CGRP and calcitonin [60].

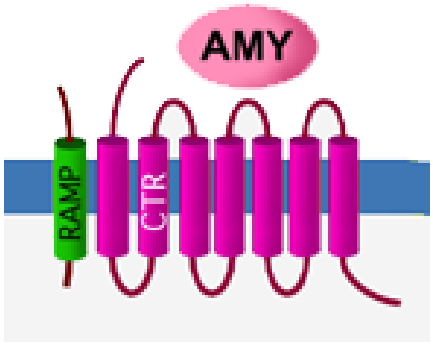

Figure 6 - Representation of the amylin receptor structure. Amy: amylin; RAMP: Receptor activity modifying proteins; CTR: Calcitonin receptor. Source: [1]

Amylin and Pain

Some studies have suggested a role of amylin in nociception; however, the research in this area has not been sufficient and the results obtained so far are often contradictory. Amylin's binding sites were described in the CNS for the first time by Sexton and his colleagues in 1994 [61]. Many of those brain areas are involved in nociception such as the nucleus of solitary tract, parabrachial nucleus, hypothalamus, the periaquedutal grey, the locus coeruleus and the dorsal raphe, and it is known that amylin is transported across the blood-brain barrier to these areas [62]. In fact, intracerebroventricular administration of amylin elicited anti-nociceptive effects in thermal acute pain, as it increased the time latency in the hot plate test response in rats [63]. Moreover, Mulder detected the presence of amylin messenger RNA and of the amylin peptide in the rat's DRG neurons, specifically in C peptidergic nociceptors, suggesting a sensorial role for this neuropeptide [64]. They also identified amylin expressing fibers in the superficial laminae of the spinal cord [64]. In fact, amylin's expression pattern in rat sensory neurons mimics that of CGRP and substance P following noxious stimulation, occurring in small to medium sized nerve cell bodies known to receive sensory input. Taking all these findings together, some research groups proposed to study amylin's role in the nervous system, more specifically in nociception.

Mulder and his colleagues continued their research in this area and studied the expression of amylin in rat DRGs after induction of inflammatory pain by intradermic injection of CFA [65]. Their results showed an increase in amylin expression at early time points, suggesting that this peptide could be involved in the initial phase of inflammation. Other important finding of this group focused on a neuropathic model in rats, which caused a decrease of amylin expression in rat DRGs as well of fiber density in the dorsal horn of the spinal cord in the ipsilateral side to the affected limb. This led

the Mulder group to consider an excitatory role for amylin under physiological conditions [66]. Accordingly, Gebre Medhin and his colleagues have confirmed that amylin is a constituent of sensory neurons in mice and its genetic ablation produced a phenotype in which mice are more tolerant to noxious stimulation. However, in the paw inflammation model induced by CFA, there were no significant differences in the ankle diameter between knock-out (KO) mice and wild-type (WT) mice [2].

On the other hand, Huang *et al* demonstrated that amylin, possibly acting on $AMY_{1(a/b)}$ or $AMY_{3(a/b)}$ receptors in the spinal cord, induced antinociceptive effects as assessed by the acetic acid writhing model of visceral pain. Some studies also show anti-nociceptive properties for salmon calcitonin (sCT), a strong amylin receptor agonist [67]. Intra-nasal sCT relieved bone pain in patients suffering from malignant tumors [68, 69] and improved pain symptoms in patients with knee osteoarthritis [70]. When centrally administered, sCT also produced strong antinociceptive effects in the tonic pain phase of the formalin test in mice [71]. It is important to note that calcitonin's expression has not been identified in the adult CNS, unlike amylin and CGRP [72]. This fact shows the relevance of amylin in pain, suggesting that salmon calcitonin may act through amylin's receptors, rather than via CTR alone, to attenuate pain.

Despite these findings on antinociceptive effects resulting from amylin-receptor activation, Bouali and his colleagues were not able to observe significant alterations in the nociceptive response when they immersed the rat's tail in a 49^{o}C water bath after central administration of amylin [73].

Interestingly, recent results obtained by our research group show that amylin administration in the rat formalin test modulates the pain behavior manifested at the interphase, when auto-analgesia in response to the noxious stimulus takes place, and in the sustained pain phase, when inflammatory processes triggered by the chemical insult are observed. This effect was dependent on the amylin dose, time of injection and route of administration [74]. It was also shown by our group that amylin's effect on pain seems to fluctuate according to the noxious stimulus nature (acute/chronic, inflammatory origin/ origin in a nerve lesion). Indeed, while chronic amylin infusion was shown to aggravate allodynia to cold stimuli in animals with neuropathic pain [75], in animals with chronic inflammatory pain induced by intra-articular CFA injection, amylin promoted analgesia [76]. These results propose an important role for amylin in nociception.

It is important to note that studies in this area are not abundant. Although some results demonstrated to be contradictory, it is settled that amylin has a role in nociception and its study can bring major progresses in pain understanding and treatment. Additionally, it is very important to determine whether overlapping or related functions of amylin and CGRP are mediated via amylin receptors or via CGRP

receptors, and to determine which are the effects specifically related to amylin's peptide and receptor.

Objectives

Amylin has been related to nociceptive mechanisms and several studies highlight amylin's role in the nervous system. However, these studies are often contradictory and limited, not looking into all the behaviors that are measurable in certain pain conditions. Other studies assessed amylin's role by intracerebroventricular administration, but these neglected the fact that amylin might have a direct peripheral effect or act at the spinal cord, especially since amylin is produced by DRG neurons. Furthermore, there are intriguing results linking amylin lack in KO mice to defective nociception [2]. The only study evaluating nociception in amylin KO mice used few pain models, did not test the effect of restoring amylin in these animals and did not investigate plastic changes in the nociceptive system of these animals. In consequence, in this project we intended to assess whether nociception and the nociceptive system were altered in animals lacking the amylin gene (KO mice).

More specifically, in this project we intended:

1) To investigate changes in the nociceptive behavior in response to noxious stimuli in amylin KO mice when comparing to their WT littermates. To achieve this goal we induced four different types of pain conditions, namely, animals were subjected to acute noxious stimuli, to visceral pain, to chronic inflammatory and neuropathic pain. The sensitivity to visceral pain as well as to standard acute mechanical and thermal stimuli was tested in naïve animals to evaluate whether nociceptive behaviors were altered in animals due to amylin´s lack. Animals ongoing inflammatory or neuropathic pain were tested with appropriate acute pain tests in order to evaluate the pain behavior changes between the two mice genotypes when submitted to the same painful condition.

2) To assess putative changes in the nociceptive system in neuronal populations of the DRG of amylin KO mice when comparing to their WT littermates. Thus, the number of neurons per area was determined as well as the neuronal density of CGRP positive neurons, as a first step towards the investigation of the type of sensory fibers that could be altered in KO mice.

3) To study amylin's effect on the nociceptive-responsive spinal cord neurons. Thus, we analyzed the c-Fos protein expression by immunohistochemistry in the dorsal horn of amylin KO and WT mice. This represented an indicator of the neuronal activity following noxious stimulation.

Methods and Materials

Animals and Habituation

For all experiments, adult amylin KO (IAPP $^{-/-}$) and WT (IAPP $^{+/+}$) littermate mice with a C57BL/6 background, bred at the Faculty of Medicine of Porto animal house, were used. The founder IAPP heterozygous F1 breeding pairs were provided by Prof. Thomas Lutz from the University of Zurich, Switzerland, in 2012. All experiments were performed with males, except the writhing test where females were used. Ear biopsies were used to tag the animal and the tissue was used for genotyping by polymerase chain reaction (PCR) analysis. DNA extraction and PCR were performed by the Laboratory of Support to Research in Molecular Medicine (LAIMM) at FMUP and are described below.

The 59 C57BL/6 mice used for the experiments were kept under controlled conditions (temperature and humidity of 22 ± 2°C and 55 ± 5%, respectively, and a light cycle of 12h light / 12 hours darkness).

The acclimatization to the conventional animal house area, where tests were performed, was of at least 7 days, during which only animal caretakers had contact with the animals. Later, the process of habituation began, with simple manipulations of the animal, such as picking them up and placing them in the test cages. Animals were habituated to the elevated cage with a grid floor used for von Frey and acetone tests, to the Hargreaves apparatus cages, as well as to the cold plate test and writhing test chambers. Moreover, animals were habituated to freely enter into the metal tube restrainer used for the tail pressure test, and to the noise of the Randall Selitto equipment used for this test. This preliminary step reduces stress, which is important to minimize confusion with stress-induced analgesia, and allows the animals to be accustomed to the noise, investigator, handling and manipulation. So, in the 4-5 days leading up to the first day of testing and just before the execution of the tests thereof, the animals were maintained for about 30 minutes in the testing room without being disturbed, and were then transferred to the test chamber where they remained for further 30 minutes without any noxious stimulation, in order to acclimatize to the conditions of the room and reduce stress and exploratory behaviors. All behavioral tests were performed during the light period for all experimental groups, in random order, in order to eliminate any change caused by the circadian cycle.

The physical condition of the animals was monitored throughout the experiment. Special attention was given to the presence of stress signs, illness or poor physical condition, such as loss or gain of excessive weight, dehydration, aggressive social behavior, low mobility, bleeding and poor wound healing, infection of the sutures and opening of the stitches in the post-surgery period.

The experimental procedures were performed according to ethical standards for the study of experimental pain in conscious animals [77], the Directive 2010/63/EU of the European Parliament and of the European Council [Strasbourg, 22 September 2010] and the rules of the regulations of local authorities [Decree-Law 129/92, Ordinance 1005/92] on the use of animals for scientific purposes.

Mice genotyping protocol

For the DNA extraction, a fresh solution of 100mM NaOH was prepared and added to the microtubes containing the mice tissue. Samples were placed in the thermocycler at 99^{o}C for about 1 hour. After cooling down, 100uL of 1M Tris HCl (pH 8) was added. After centrifugation, a 1 µL aliquot of the extracted DNA was used for the polymerase chain reaction (PCR). To each PCR tube was further added the following solutions from the Citomed BM-10002 KIT: 0.1 µL Taq polymerase, 2 µL of Buffer and 2µL of MgSO4 (2 mM,). Finally, 1 µL of each primer (at 10 µM) was added, namely, primer 206: 5'-CTTGGGTGGAGAGGCTATTC-3', primer 207: 5'-CACAGCTGCGCAAGGAAC-3', primer 208: 5'-GTAGCAACCCTCAGATGGAC-3' and primer 209: 5'-GAGGACTGGACCAAGGTTGT-3', all produced by Stab Vida.

The samples were placed in a thermocycler, which conducted 35 cycles of reaction. Each cycle included 5 minutes at 95^{o}C, followed by 30 second at 95^{o}C, 62^{o}C and 72^{o}C, and finally 10 minutes at 72^{o}C. At last, the samples were run in an agarose gel for electrophoresis. The amplified target sequences included a mutated allele with 200 base pairs (knock-out mice) and a wild-type allele with 100 base pairs (wild-type mice). When both products were found in the gel, the sample belonged to a heterozygous mouse, as we can see in the following gel-example (Figure 7).

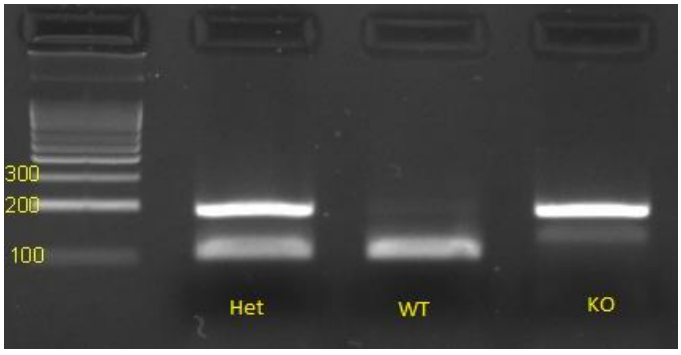

Figure 7 - Agarose gel. Het- heterozygote mice; WT- wild-type mice (100 base pairs); KO- knock-out mice (200 base pairs).

Visceral Pain: Writhing test induced by intraperitoneal acetic acid injection

The acetic acid-induced visceral pain model is widely used in experimental research to produce a writhing reaction, characterized by contraction of the abdominal musculature and extension of the hind limbs (Figure 8), associated with visceral pain [24]. Animals were placed in the test chamber, a clear 20 × 26 × 12 cm plastic cage (figure 8), for 10 to 15 minutes to acclimatize. Following the intraperitoneal injection of 1% acetic acid (10ml/kg of body weight; Sigma-Aldrich, [24]), animals were placed back into the test chamber and were video-recorded for twenty minutes. Behavior was analyzed later with the program Etholog 2.25 [78]. The number of writhes was monitored for twenty minutes and recorded in five minutes intervals [24]. The total number of writhes between 5 and 15 min after injection [51, 79] and the latency time to the occurrence of the first writhe were also assessed.

Figure 8 - Contraction of the abdominal musculature and extension of the hind limbs.

Induction of Chronic Inflammatory Pain: Complete Freund's Adjuvant Model

The animals were anesthetized with volatile anesthesia (isoflurane), at first in a glass chamber at 4% (to induce) and then directly on the nose at 1.5% (to maintain). Then, animals received an intraplantar injection of 20 µL of Complete Freund's adjuvant (CFA) into the left hind paw. The injection was performed slowly to avoid the reflux of CFA. The CFA solution consists of water in oil emulsion containing killed and dried *Mycobacterium butyricum* (Difco Laboratories [80]; see composition in annex).

The inflammation reaction was monitored daily using a scale that takes into account the animal's behavior and local inflammation signs. The inflammatory scale considered has the minimum value of zero, where the animal shows no signs of inflammation, and the maximum value of four, where the animal demonstrates severe inflammation and persistent flexion of the paw [81].

Mice were transferred to the behavioral testing room at least one hour before testing to acclimatize. The von Frey and Hargreaves behavioral tests (see below) were performed at three hours, one day and two days after injection. Both hind paws were tested.

Induction of Chronic Neuropathic Pain: spared nerve injury (SNI) model

The spared nerve injury surgery in mice was performed in order to induce a painful neuropathy, as described by Richner *et al.* [82] which is based on the procedure defined by Decostered and Woolf [19] in rats.

Briefly, the animals were anesthetized using the combination of Domitor (1 mg/kg, medetomidine hydrochloride) with Imalgene (75 mg/kg, Ketamine hydrochloride) diluted in distilled water and administered intraperitoneally. The left thigh was shaved and disinfected with Betadine and 70% ethanol. A 1 cm incision was made in the skin in the longitudinal direction proximal to the knee, subsequently detaching the skin from the underlying connective tissue layer covering the muscle. The muscle layer was separated with the help of blunt scissors, right next to the clearly visible blood vessel, close to the thigh bone (femur). At this point, a stereo microscope was required so the sciatic nerve and its different branches (tibial, peroneal and sural) could be visualized. A silk suture (6-0, No. 18020-60, Fine Science Tools) was applied around the tibial and peroneal branches, and a tight surgical knot was made, leaving the sural branch intact. Both nerves (tibial and peroneal) were held with a sterile tweezer bellow the suture and a 1 mm portion was cut with a small scissor. The muscle layer and the skin were sutured using absorbable 4-0 suture (simple knots in the muscle layer and U-eversion knots in the skin; C1048213, Safil, Braun) and lidocaine was applied to minimize local discomfort. After surgery, the wound was disinfected, the animals were rehydrated with a subcutaneous injection of 0.5 mL of saline solution (0.9 % NaCl) and finally, the anesthesia was reverted with a subcutaneous injection of Antisedan (atipamezol, 1 mg/Kg). In the days after surgery, easy access to water and food were provided. The von Frey, Acetone and the Hargreaves behavioral tests (by this order, see details of the tests below) were performed one day before surgery and on day one, three, seven and fourteen after surgery. The Cold Plate test was performed just on day 14 of SNI (see details below) after the other three tests.

Acute pain behavioral tests

These tests were applied to naïve mice and some were also used to assess the development of allodynia and hyperalgesia in chronic pain animals, as mentioned above. Acute pain tests were performed in naïve animals to detect differences in acute

sensitivities between both genotypes. The tail pressure and cold plate tests were performed in these animals to assess mechanical and cold hyperalgesia, respectively.

To assess acute mechanical sensitivity and heat hyperalgesia in naïve animals, the von Frey and Hargreaves tests were performed, respectively, at the baseline time point of the CFA animals (before CFA injection), since at baseline all the animals were naïve.

Von frey

Mechanical allodynia was assessed both in naïve and in chronic pain animals using a set of calibrated von Frey filaments (Figure 9B; Touch test sensory evaluator kit, Stoelting). Starting from the thinnest hair, each filament was applied on the plantar surface of the hind paw (Figure 9A) (for naïve and CFA-mice) or on the lateral area of the hind paw (innervated by the spared sural nerve for the SNI-mice) five consecutive times for thirty seconds until a response was observed. A response was considered positive if the mouse licked or removed the paw from the platform in response to the application of the filament. Both paws were tested. The threshold was considered as being the lowest filament force that provoked a paw withdrawal response (adjusted from [83]).

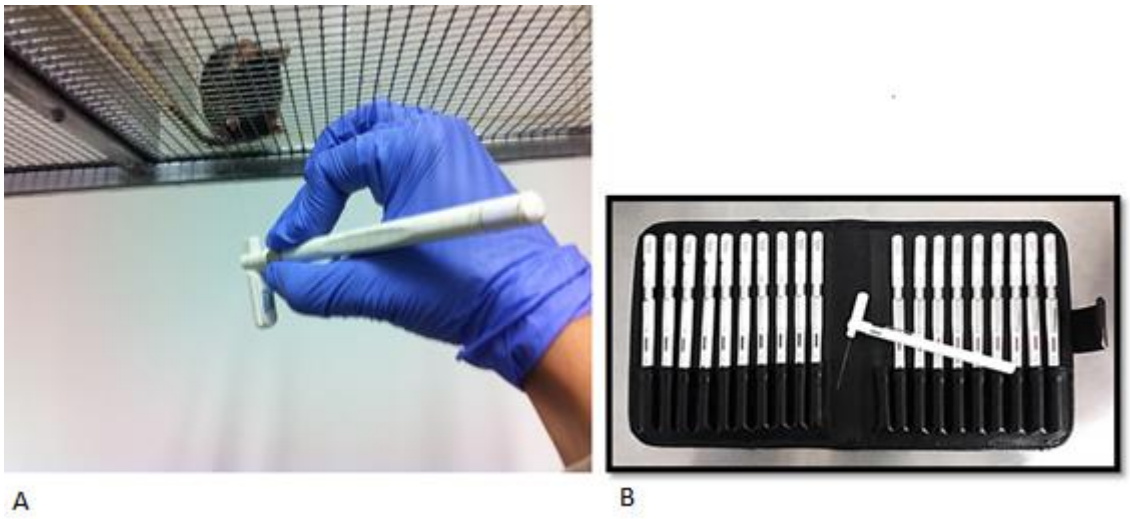

Figure 9 - A) Von Frey test. B) Calibrated von Frey filaments.

Tail Pressure

In naïve animals, mechanical hyperalgesia was assessed by only using the tail pressure test [84]. The animals were introduced in the metal restrainer, leaving the tail out and loose in order to place it on a small platform under the conic tip of the Randall Selitto apparatus (Figure 10) (Ugo Basile, Biological Research, Comerio). Pressing the apparatus pedal, an increasing force was applied to the animals' distal tail portion (about 1-2 cm from tail tip), until the first pain response was observed. A response was considered positive if the mouse struggled, squeaked, or tried to remove the tail from

the platform. The force that elicited the noxious reaction was noted. In the absence of any reaction, a 250 g cut-off value was used to avoid tissue damage. The procedure was repeated, so that two measures were taken per animal. The nociceptive value (grams) for each mouse was taken as the mean value of two consistent measurements.

Figure 10 - Randall Selitto apparatus.

Cold plate

This test was used to assess the sensitivity to noxious cold (adapted from [85]). Naïve mice were placed on a 0 °C metallic plate, surrounded by an acrylic chamber (figure 11) (Hot/cold plate apparatus, Bioseb, France) so that the animals were restricted to move only on the plate area and their behavior was recorded for 120 seconds. Two parameters were measured: the latency to hind paw flinching/flicking, licking, or jumping was measured at the time of testing by the device, and the number of times the animal flinched the hind paws during the 120 seconds period which was evaluated later by video analysis using the software Etholog 2.25 [78]. To evaluate thermal hyperalgesia in the 14 day SNI-mice, the plate was set to a temperature of 5 °C instead, and the evaluation of the latency of response was confined to the hind paw ipsilateral to the nerve lesion. The animals' behavior was video-recorded for 300 seconds for analysis of the total number of flinches with Etholog 2.25, as explained above.

Figure 11 - Cold plate test.

Hargreaves

The mice were placed in the Hargreaves apparatus (Figure 12) (Plantar test # 37370, Ugo Basile, Biological Research, Comerio), which was designed with the purpose of allowing the assessment of thermal allodynia and hyperalgesia in the paws (adapted from [86]). Using an infra-red setting of 50 units and a cut-off time of 15 seconds to avoid tissue damage, three to four measurements were obtained for each hind paw. In naïve and CFA-mice, the laser beam was directed to the middle of the plantar region of the animal's hind paw whereas in SNI-mice the hypersensitive lateral area of the paw was targeted. The latency of both paws was measured. For each mouse 3-4 readings were obtained during a period of 30 min (5-10 min interval) and the mean latency of 3 consistent measurements was used for analysis.

Figure 12- Hargreaves test.

Acetone

The acetone test allows evaluating thermal allodynia, and was only performed in SNI-mice. A syringe with a piece of rubber tubing attached to its end was filled with acetone and the plunger depressed so that a small drop of acetone formed at the top of the tubing. The syringe was raised to the hind paw from below, depositing the acetone drop on the hypersensitive lateral-external part of the hind paw (Figure 13). The total duration of time of lifting, licking, flinching, shacking, and rotating of the torso was determined with the help of a chronometer. If necessary, the procedure was executed again 5 minutes later. If the animals did not respond to two measurements, it was assumed a minimum response value of 0.5 seconds, considered the normal response (adapted from [87]).

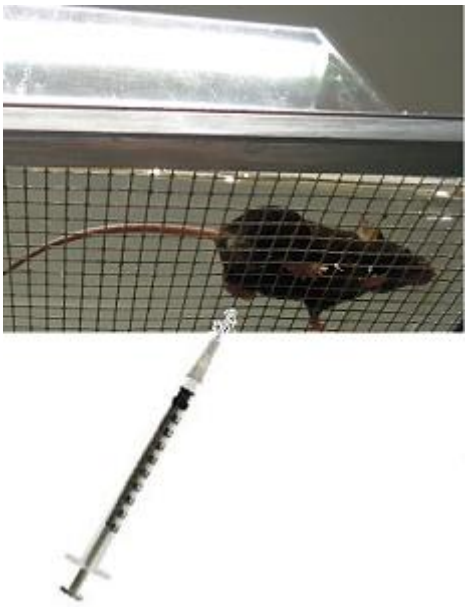

Figure 13 - Acetone test.

Perfusion, fixation and dissection of the biological material

All the animals from the different pain models were perfused two hours after the beginning of the last acute behavioral test performed, when c-Fos expression is thought to achieve the peak. The animals were injected in the intraperitoneal cavity with diluted Eutasil® (67 mg/Kg sodium pentobarbital in 0.9% saline solution). In order to perfuse the mice, both abdominal and thoracic cavities where opened and the heart was exposed. An incision was performed in the left atrium with the help of a scissor to allow the blood to flow out. Afterwards, a needle was introduced into the left ventricle, allowing the washing solution (Tyrode's pH 7.2) and the tissue fixative to circulate and leave the organism. The tissue fixative was a solution containing 4 % of

paraformaldehyde diluted in a phosphate buffer (pH 7.2). Naïve animals were perfused in a similar way.

At the end of the perfusion the animals' tissues were carefully dissected. For naïve mice and animals from the chronic inflammatory pain and neuropathic pain models, the brain and the segments L3-L6 of the spinal cord as well as the associated L4 and L5 DRG were collected. For the animals from the visceral pain model, the segments T5 to L2 were collected, as well as the brain. The biological material was post-fixed for 4 hours, in paraformaldehyde 4% at 4^{o}C, and then cryopreserved in 30 % sucrose with azide (to prevent microbial contamination) for, at least, 48 hours.

Processing and sectioning of the biological material

The DRGs were separated from the spinal cord and kept in 30 % sucrose with azide until further use. A precise incision was performed in the contralateral side of the ventral horn of the spinal cord in relation to the affected paw, in the case of CFA and SNI-mice, to allow a clear distinction between both sides of the spinal cord and the identification of the ipsilateral dorsal horn. The spinal cord of the animals from the visceral pain remained intact, as it was not necessary to discriminate spinal cord sides in this case.

The spinal cords were frozen and transversely sectioned in four consecutive series of 30 µm thickness sections in the freezing microtome (Leitz, Barcelona). The obtained slices were transferred into a cryoprotector solution and preserved at -20^{o}C for subsequent immunohistochemistry reactions.

The DRGs were sliced with a 10 µm thickness in the cryostat (Leica, Germany). They were collected in glass slides in three (L4) or four (L5) consecutive series. After thawing the sections on the glass slides at 37^{o}C for 1h the slides were kept at-20^{o}C for tissue preservation until subsequent immunohistochemistry processing.

Immunohistochemistry reactions

Anti-amylin in DRGs

The immunohistochemistry reactions for detection of amylin expression in L4 and L5 DRGs of naïve mice were performed on the glass slides. Two hours before the reaction, the slides were re-heated in a plate at 37 ^{o} C to defrost the tissue. The sections were washed with phosphate buffered saline (PBS) 0.1 M and with a solution of PBS with Triton-X100 (PBST), and were then blocked for 1 hour in a blocking solution containing 10% normal horse serum (NHS) in PBST. After blocking, the sections were

incubated overnight at room temperature in a PBST solution containing 2% of NHS and the polyclonal primary antibody against amylin made in rabbit (1:800 Bachem T-4146).

Afterwards, sections were washed and incubated in the secondary antibody donkey anti-rabbit alexa-488 (1:1000; A21206, Molecular Probes) in PBST for 1 hour at room temperature. The sections were subsequently washed with PBST and PBS and finally were mounted using glycerol phosphate as mounting media.

Anti CGRP in DRGs

The immunohistochemistry reactions for detection of CGRP expression in L4 and L5 DRGs of naïve mice were performed on the glass slides. Briefly, the immunohistochemistry reactions followed the same steps as the anti-amylin reactions, excepting the incubation in the primary and secondary antibodies. In this case, the sections were incubated in polyclonal primary antibody against CGRP made in sheep (1:1000 BML-CA1137, Enzo) and in the secondary antibody donkey anti-goat alexa-488 (1:1000 A11055, Molecular Probes).

Anti c-Fos in spinal cord

C-Fos expression in the spinal cords was determined by an immunohistochemistry reaction in free-floating sections. This reaction was performed in segments L3 to L6 in the neuropathic model, since these are responsible for processing information from the hind paws. For the visceral pain model, the spinal cord segments T5 to L2 were used, as these receive the primary afferent fibers that transmit information relating to the internal peritoneal organs.

For the immunohistochemistry reaction, the spinal cord sections were transferred to cell culture plates and washed with PBS 0.1 M. In order to block the endogenous peroxidase activity, the tissue was incubated with a solution of 1% hydrogen peroxide (H_2O_2) in PBS for 15 minutes. After washing with a solution of PBST, the sections were incubated for 90 minutes at room temperature with a blocking solution containing 10% normal swine serum (NSS) in PBST to prevent antibody binding to nonspecific antigenic sites. Spinal cord sections were subsequently incubated with a polyclonal antibody anti-c-Fos made in rabbit (ABE457, MerkMillipore) at a dilution of 1:1000 in PBST with 2% NSS for 48 hours at 4 °C.

Then, sections were incubated at room temperature with a secondary biotinylated IgG anti-rabbit (Dako, Glostrup) made in pig diluted in a ratio of 1:200 in PBST 2% NSS for 75 minutes. Following 1 hour incubation in an avidin-biotin-peroxidase complex (ABC kit, Vectastain, Peterborough) solution, to amplify the signal four-fold, sections were equilibrated in a 0.05 M Tris-HCl pH 7.6 solution before the reaction with 3,3-diaminobenzidine (DAB; Sigma Aldrich) diluted in the same buffer containing 0.025% H_2O_2. The oxidation of the DAB due to the peroxidase action

produced a brown precipitate in the antigen-antibody reaction sites. The reaction was then stopped by washing the tissue with Tris-HCl 0.05M pH 7.6 solution again. All steps were performed under moderate agitation. After the immunohistochemistry reaction, sections were placed in gelatin-coated slides and left at 37 °C overnight to dry. The next day, they were cleared in xylene (Prolabo Carnaxide) for 1 minute, covered with mounting medium (Entellan; Merk, Germany) and cover-slipped.

Histological Hematoxylin-Eosin staining

In order to quantify the number of L4 and L5 DRG neurons from naïve WT and amylin KO mice and measure their cell body areas, an histological staining with hematoxylin and eosin (H&E) was performed to label all the cell bodies in the DRG sections.

Briefly, the DRG slices were hydrated with tap water. Then, the slices were dipped in hematoxylin solution for about 90 seconds. Sections were then washed with water again before counter-staining with eosin for about 30 seconds. The slices were washed again and then dehydrated sequentially in a 90% ethanol solution and then absolute ethanol. Sections were then cleared in xylol and mounted with Entellan.

Quantification of c-Fos-positive neurons in the spinal cord

The sections immunoreacted against c-Fos were analyzed using an optical microscope (Leica) coupled to a digital camera (Leica camera) and specific computer image software (LAS 4.6- Leica Application Suite). Per SNI-animal, 8-10 slices from segments L3 to L6 were chosen and for visceral pain animals, 10-12 sections from T5 to L2 region of the spinal cord were selected for analysis. The selected slices were photographed and then the c-Fos positive nuclei were counted in the captured images by using Image J software version 1.37 (free access software).

The central canal was used as a marker to divide the spinal cord into its dorsal and ventral parts. The nuclei positive for c-Fos were quantified only in the dorsal horn ipsilateral to the paw subject to the SNI surgery in the animals from the neuropathic pain model (Figure 14 A). The expression of c-Fos in the spinal cord sections from the animals of the visceral pain model was quantified in both dorsal horns (Figure 14B).

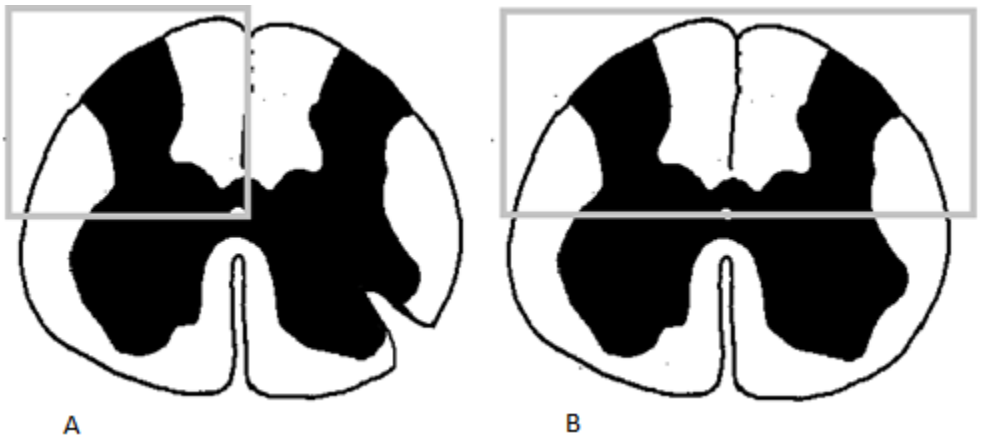

Figure 14 - Illustration of the spinal cord region considered for quantification of c-Fos. A) considered area for the neuropathic pain model. B) considered area for the visceral pain model.

The average of the number of cells positive for c-Fos in each analyzed area was used for statistical analysis.

Quantification of CGRP-positive neurons and determination of neuronal cell body areas in DRGs of WT and KO mice

Immunohistochemistry analysis of L4 and L5 DRGs was performed using a fluorescence microscope (AxioImager Z1; Zeiss) coupled to a digital camera (AxioCam MRm) and computer image software (AxioVision 4.6) to capture the images.

The total number of neurons, as well as the number of CGRP-positive neurons, per section, was counted using ImageJ software. This allowed calculating the percentage of CGRP-positive neurons.

The neuronal cell body areas of CGRP positive cells and neurons from the L4 and L5 DRGs from naïve animals were measured, in order to evaluate possible changes in the CGRP-positive neuronal population and in the global neuronal population in the two different groups of animals (WT vs. KO). Neurons were manually outlined in the captured images in the computer and the area was measured using the Image J program version 1.37 (free access software). Cell areas were grouped into three categories: small (<600 μm^2), medium (600-1200 μm^2) and large area neurons (>1200 μm^2) according to Negri et al [88].

Statistical Analysis

Statistical analysis was performed using Prism software (version 5, GraphPad, California). The results were presented as mean ± standard error of mean (SEM) for each experimental group. The analysis of data normality was assessed by the Kolmogorov-Smirnov test and, whenever any of the experimental groups did not

present the expected Gaussian curve, the appropriate non-parametric tests were performed. If the data followed a Gaussian curve, parametric tests were done. The Grubb's test was also performed in order to detect outliers when a result seemed to diverge substantially from the rest of the group. Data from the cold plate and tail pressure tests were analyzed by the Student's unpaired t test to compare the two groups in the study. The nonparametric Kruskal-Wallis test was used to test the differences at each time point between experimental groups on data from the von Frey test, as the results appear in a logarithmic scale (force exerted by von Frey filaments).

For data relative to the acetone, the Hargreaves and the Writhing tests throughout time, two-way analysis of variance (Two-way ANOVA) was used with repeated measures (time as repeated measure, in minutes or days) followed by the post-hoc Bonferroni test for the analysis of punctual differences.

The percentage of CGRP-positive neurons in the DRGs and the different area distributions, in both hematoxylin-eosin stained and CGRP immunoreacted sections, was statistically analyzed by the Student's unpaired t test. This test was also used to analyze data regarding the quantification of c-Fos expression in the spinal cords.

In all statistical analysis p values < 0.05 were considered as significant.

Results and Discussion

Acute pain tests

Acute tests performed on naïve animals

Naïve animals, both knock-out for the amylin gene and wild-type animals were tested on acute pain behavioral tests in order to understand amylin's role in acute nociceptive transmission.

The von Frey test was conducted in order to assess differences in mechanical allodynia between WT and amylin KO mice (Figure 15). WT animals responded to filaments which induced forces around 0.27±0.09 g, while KO mice responded to filaments which induce lower forces, in the average of 0.12±0.05g. However, the Mann Whitney test performed did not detect a statistical significant difference between both groups. The values observed in WT mice are consistent with those obtained in previous studies in mice ([89]), where wild-type mice showed a threshold of 0.29±0.04g.

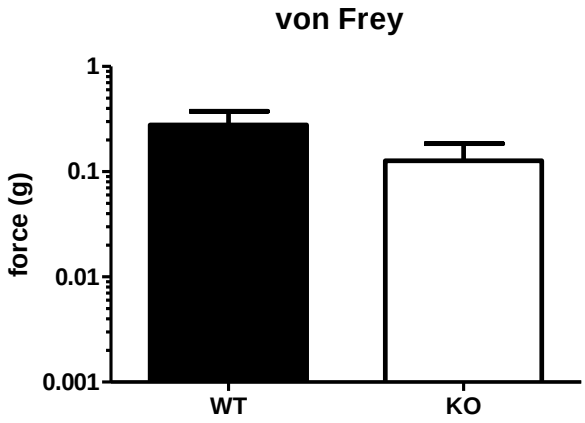

Figure 15 - von Frey test in the plantar surface of KO and WT naïve mice hind paws. WT n = 5, KO n = 6.

The tail pressure test was performed to assess mechanical hyperalgesia. As we can observe in Figure 16, amylin KO animals responded to significantly lower forces (7.73±0.84g) when comparing to WT animals which showed responses to average forces of 10.88±0.62g ($p<0.05$). The results from both mechanical tests are in agreement and suggest that, in normal conditions, amylin KO mice are generally more sensitive to mechanical stimuli than WT mice.

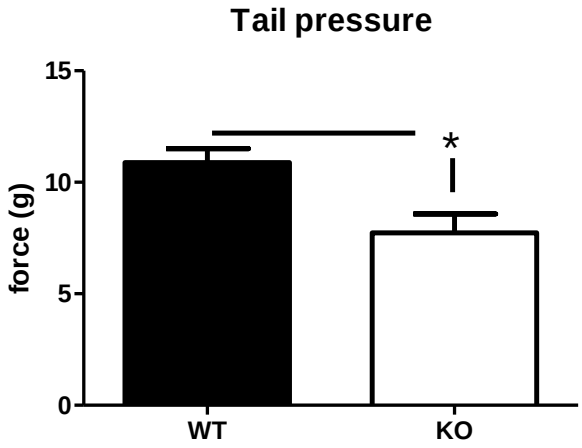

*Figure 16 - Tail Pressure test in KO (n = 8) and WT (n = 6) naïve mice; *p<0.05*

The Hargreaves test was also performed in these animals to assess thermal hyperalgesia. There were no significant differences between the two animal groups which suggest that amylin KO mice do not have altered sensitivities to noxious heat (Figure 17). Even though this would suggest that amylin is not involved in the mediation of noxious heat stimuli, there are previous studies showing an antinociceptive effect upon intracerebroventricular amylin administration in the hot plate test [63], which highlight a central modulatory role.

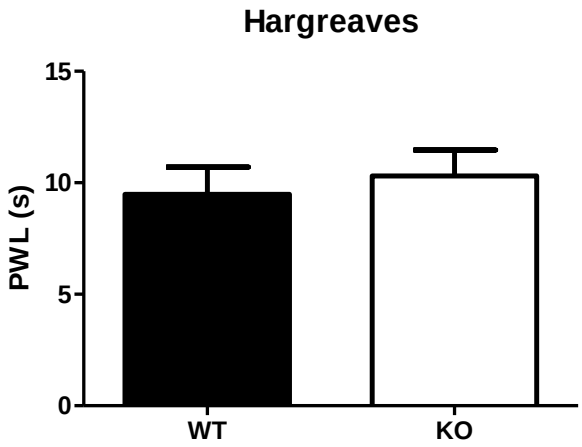

Figure 17 - Hargreaves test in WT (n=6) and KO naive mice (n=6). Paw withdrawal latency (PWL) of WT and KO mice hind paw.

The cold plate test was performed to determine cold hyperalgesia. The paw withdrawal latency was measured in both KO and WT naïve animals. When analyzing the results obtained, we observed that one of the animals exhibited an abnormal response that differed significantly from the other animals of the group. The Grubbs' test confirmed that this value was a significant outlier in the group (Figure 18) and thus this value was not considered for further statistical analysis.

Row	Value	Z	Significant Outlier?
1	17.000	0.38454	
2	20.000	0.29075	
3	14.000	0.47833	
4	19.000	0.32201	
5	120.000	2.83559	Significant outlier. P < 0.05
6	19.000	0.32201	
7	19.000	0.32201	
8	25.000	0.13443	
9	20.000	0.29075	
10	20.000	0.29075	

Figure 18 - Grubb's test result for the data regarding the cold plate test in KO and WT naïve mice.

The results of the cold plate test are represented in Figure 19). As can be observed, amylin KO animals elevated the hind paw lesser times than WT animals (18.33±2.911 flinches in WT *versus* 15.00±2.99 flinches in KO mice; Figure 19A), although the differences were not statistically significant. Furthermore, KO animals elevated the hind paw significantly later than the WT animals (PWL of 13.00±1.15 seconds in WT *versus* 19.22±0.96 seconds in KO mice; $p<0.05$; Figure 19B) in response to the cold stimulus. Though the first result is not significant, it is in agreement with the second result, both suggesting that KO animals tolerate better the noxious cold than WT animals.

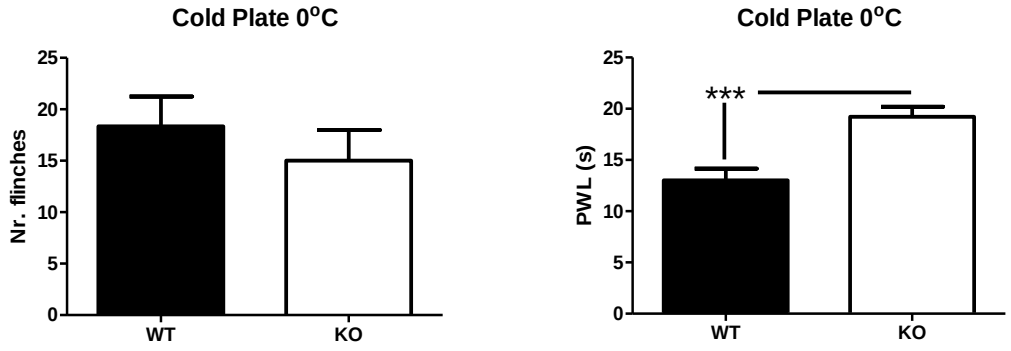

A B

*Figure 19 - Cold plate test in KO (n=10) and WT naïve mice (n=9). A) number of flinches; B) paw withdrawal latency. ***p<0.05*

It is interesting to note the dissimilarities in results when analyzing both thermal acute and mechanical acute pain tests. It is possible that the ionic channels working as detectors of cold stimuli are altered in KO mice, since they respond to noxious cold in a different manner compared to WT animals. The channels responding to cold include transient receptor potential melastatin 8 (TRPM8) [26], and are

expressed by A and C fibers [90], [84] that mediate cold stimuli and can be differentially expressed by these nociceptors. On the other hand, the ionic channel responsible for sensitivity to noxious heat is transient receptor potential vanilloid 1 channel (TRPV1) and is almost exclusively expressed in C peptidergic nociceptors ([90], [84]). It is possible that the expression of these channels remains intact in KO mice, since they respond to heat practically the same way as WT animals. Taken these results together, it is reasonable to hypothesize that the expression patterns of TRPM8 and/or that the A fibers on amylin KO mice may be altered.

Inflammatory pain model

The induction of inflammatory pain by CFA injection in the plantar paw elicited a strong immune response that resulted in a localized arthritic reaction. Indeed, both WT and KO mice developed a severe inflammation within the first three hours after injection, associated with adaptive postural changes, namely with persistent flexion of the paw, confirming the induction of the inflammatory pain model. This was reflected in an increased inflammatory score which reached values of 3.33±0.27 at 3 hours and remained significantly high until 2 days after CFA injection (Figure 20). The associated inflammation induced-nociceptive behavioral changes, which included mechanical allodynia and thermal hyperalgesia, were observed in both animal groups. As it was expected, the contralateral hind paw remained uninflamed in both genotypes. The lack of differences in paw inflammation between genotypes was expected, as it was already observed by Gebre-Medhin and colleagues that amylin KO mice had similar ankle joint diameters at different time points after intra-plantar CFA-injection, as WT mice [2].

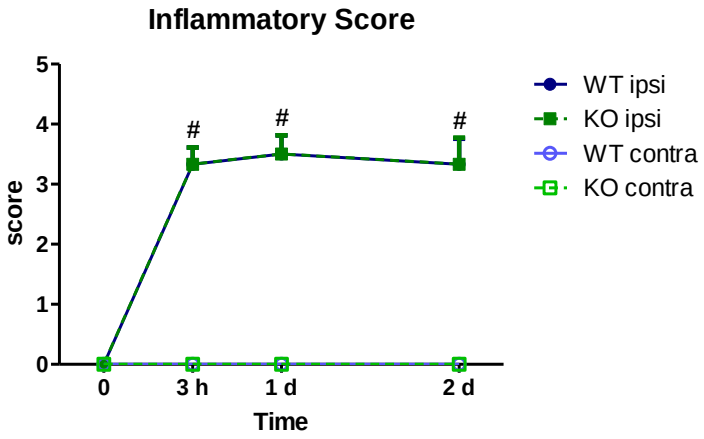

Figure 20 - Evolution of inflammation in WT-CFA (n=6) and KO-CFA (n=6) animals. #p<0.001- WT and KO ipsilateral hind paws vs. WT and KO contralateral hind paws.

In the von Frey test, the mean forces that provoked a noxious response in the WT animal group before inflammation induction (day 0) were of 0.27±0.09g. On the other hand, amylin KO animals generally responded to filaments exerting lower forces,

which were around 0.19±0.08g. Despite this tendency for the amylin KO animals to be more sensitive to mechanical forces, there were no significant differences between the two groups, at day 0 ($p>0.05$; Figure 21).

From three hours after injection until the end of the behavioral tests, we observed that the forces required to induce the contralateral hind paw withdrawal did not vary much, as expected, although we could note a slight increase in the KO animal group to values that were similar to the WT group (Figure 21).

As predicted, all animals showed a decrease in the forces required to induce ipsilateral hind paw withdrawal after CFA injection in comparison to the contralateral hind paws (Figure 21), confirming the development of mechanical allodynia. Even though there were no significant differences regarding the forces supported by the ipsilateral hind paws between WT and KO mice, we could observe that KO animals tended to respond to greater filament forces, at 3h and 2 days of inflammation, indicating that KO animals may have a tendency to develop less mechanical allodynia in inflammatory pain conditions. However, this was just a trend, without statistical significant alterations in the way the two animals groups answer to the mechanical stimuli.

The Kruskal Wallis test at each time point demonstrated only a significant difference between the WT ipsilateral hind paw and the KO contralateral hind paw (0.038±0.03g and 0.26±0.05g, respectively, $p<0.05$, Figure 21). The lack of significance when comparing to its own control (WT contralateral paw) is probably due to the large variability found within the groups, and to the relatively low number of animals tested. Thus, the ipsilateral hind paws from amylin KO animals tended to respond to similar forces when compared to both WT and KO non-damaged hind paws, contrarily to what happens to the ipsilateral hind paws of WT animals, which responded to lower force filaments.

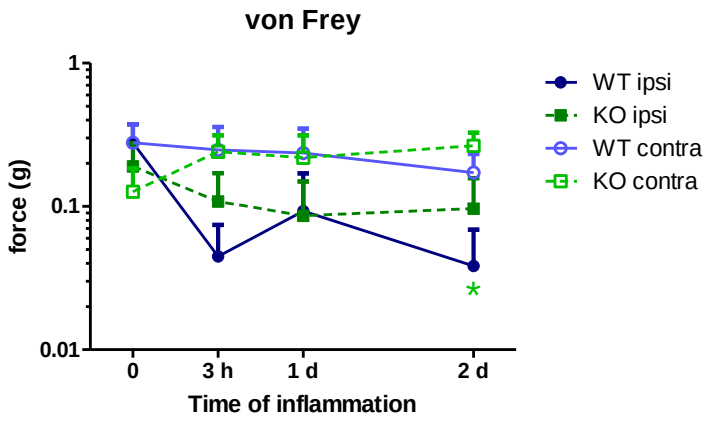

*Figure 21 - Mechanical allodynia evolution in WT (n=5) and KO mice (n=6) after CFA injection. *p<0.05- WT ipsilateral hind paw vs. KO contralateral hind paw, after 2 days of CFA injection.*

Our group found that chronic amylin administration promoted analgesia in rats that received intra-articular CFA injection (monoarthritic rats). Specifically, there was an attenuation of mechanical allodynia and hyperalgesia on days 7 and 13 of inflammation [76]. The abovementioned tendencies found in the von Frey test in mice lacking amylin are difficult to reconcile with the antinociceptive effects found upon chronic amylin administration in monoarthritic rats [76]. Still, one has to keep in mind that amylin KO mice do not express amylin constitutively, that is, since the embryonic phases of development. Therefore, the effects observed in amylin KO mice are not only a consequence of a temporary amylin lack, as a neuropeptide modulating pain, but rather the outcome of its permanent lack which may have affected the nociceptive system development, as further discussed later.

Mulder and colleagues found an increase in amylin's expression in rat L5-DRG at early time points of paw inflammation [91]. One could hypothesize that the small trends found in the responses in the von Frey test could be associated with the fact that amylin KO mice cannot overexpress amylin in response to inflammation.

In order to assess thermal hyperalgesia in the chronically inflamed animals, the Hargreaves tests were performed. The hind paw withdrawal latency (PWL) to the hot beam was measured for both hind paws of both animal groups. The 2 way ANOVA statistical analysis performed along time showed that both animal groups presented a similar PWL around 9-10 seconds in both hind paws, (10.35±1.58s for the ipsilateral and 9.48±1.22s for the contralateral hind paws in WT mice; 9.60±1.32s for the ipsilateral and 10.30±1.16s for the contralateral hind paws in KO mice), at day 0 (baseline), as expected (Figure 22).

In the non-damaged hind paw (contralateral), we did not detect any difference over time in any of the genotypes. As it was expected, the PWL in the ipsilateral hind paws decreased significantly at 3 hours after CFA injection in both animal groups (3.14±1.08s for the WT and 2.97±1.22s for the KO groups) ($p<0.05$), confirming that the model was well induced. At this time point, there were no differences between the two different genotypes comparing both ipsilateral hind paws, and the same happened at 1 and 2 days after CFA injection, which suggests that amylin plays no role in the response to noxious heat in inflammatory pain conditions. There were significant differences in the PWL values between the ipsilateral hind paws and the WT contralateral hind paw group on day 1 of inflammation (WT ipsilateral, $p<0.01$; KO ipsilateral, $p<0.05$: Figure 22), confirming that mice from both genotypes exhibited thermal hyperalgesia. However, we could note a slight tendency for KO animals to progressively increase their PWLs over time, since on day two, the ipsilateral hind paws of WT animals showed significantly lower PWLs comparing to KO contralateral paws. At this time, it was detected a tendency for the KO animals to exhibit higher PWLs in

their ipsilateral hind paws, which suggests that, at later stages of inflammation, KO animals might be less hypersensitive to thermal stimuli.

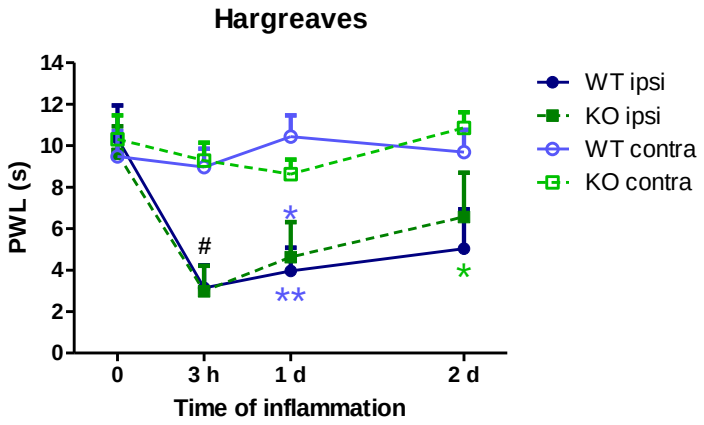

*Figure 22 - Thermal hyperalgesia and allodynia evolution for KO (n=6) and WT (n=6) animals after CFA injection. # p<0,01 WT and KO ipsilateral hind paw vs. WT and KO contralateral hind paw, at 3 hours after CFA injection. **p<0.01 WT ipsilateral hind paw vs WT contralateral hind paw, one day after CFA injection. *p<0.05- KO ipsilateral hind paw vs. WT contralateral hind paw, one day after CFA injection. *p<0.05-WT ipsilateral hind paw vs. KO contralateral hind paw, 2 days after CFA injection.*

Overall, the KO mice seemed to develop less allodynia and hyperalgesia upon this chronic inflammatory condition but significant differences between genotypes were not detected. However, as WT ipsilateral hind paws presented significant differences to non-damaged hind paws, contrarily to KO ipsilateral hind paws, this could indicate that WT mice were, in general, more responsive to the noxious stimuli applied. Due to technical problems, it was not possible to process the biological tissue of these mice, so it was not possible to support these results with the immunohistochemical analysis of c-Fos expression in the spinal cord.

The differences between genotypes could become more evident with a higher number of animals per experimental group, which would allow developing more solid conclusions regarding the role of amylin in inflammatory pain.

Pathological Pain Models: Neuropathic Pain

The induction of neuropathic pain by using the spared nerve injury model resulted in long-lasting and intense allodynia and hyperalgesia in the lateral surface of the hind paw receiving innervation from the injured nerve. The nociceptive responses of both hind paws were evaluated on day -1 (baseline), and days 1, 3, 7 and 14 after SNI surgery by the von Frey, acetone, Hargreaves and cold plate tests.

In the von Frey test, both animal groups responded to similar filament forces at day -1 (0.33±0.10g for the ipsilateral and 0.38±0.12g for the contralateral hind paws in WT mice; 0.36±0.04g for the ipsilateral and 0.4±0.00g for the contralateral hind paws in KO mice; Figure 23). As it was expected, the force required to elicit a response significantly decreased from day one after surgery in the ipsilateral hind paws of both

animal groups (Figure 23), confirming the occurrence of mechanical allodynia. However, WT animals responded to statistically significant lower forces when their ipsilateral paws were stimulated, as compared to data from the contralateral hind paws of both groups ($p<0.05$), while KO animals did not (ipsilateral KO vs. contralateral WT or KO, $p>0.05$ for days 1 and 3).

At days 1 and 3, it became very evident that KO mice displayed less allodynia to mechanical stimuli (0.04±0.01g for the ipsilateral hind paw and 0.28±0.05g for the contralateral hind paw at day one and 0.05±0.02g for the ipsilateral hind paw and 0.34±0.05g for the contralateral hind paw at day 3), unlike WT mice which presented significant differences from their internal controls (non-injured contralateral hind paws) (0.008±0.00g for the ipsilateral hind paw and 0.25±0.08g for the contralateral hind paw at day one and at day 3).

However, at day 7 and 14 after surgery, the affected hind paws of both animal groups exhibited significant differences in von Frey test responses (0.008±0.00g for the WT mice and 0.02±0.005g for KO mice) comparing to the contralateral hind paws of KO animals (which responded to mean values of 0.22±0.05g). Although the KO ipsilateral hind paws also showed a significant difference in response comparing to the contralateral hind paws response of KO mice, these differences were significantly smaller ($p<0.05$; Figure 23) than those presented by WT animals ($p<0.01$; Figure 23). Data obtained for WT animals are in agreement with results previously described, before and after SNI surgery in mice [92].

Even though there were no significant differences in the response when comparing the hind paws in the same condition between both genotypes (WT ipsilateral vs. KO ipsilateral and WT contralateral vs. KO contralateral), it was detected a tendency for KO animals to elicit a noxious response only when higher force filaments were applied.

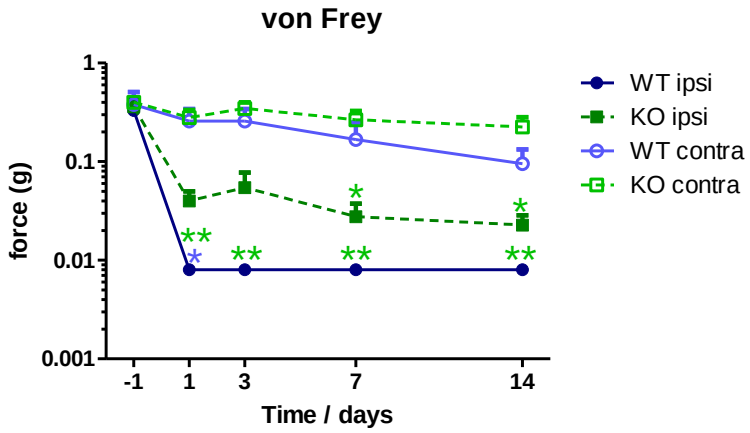

*Figure 23 - Mechanical allodynia progression for WT and KO mice after SNI surgery. *p<0.05- WT ipsilateral hind paw vs. WT contralateral hind paw, at day 1 after SNI surgery. **p<0.05-WT ipsilateral hind paw vs. KO contralateral hind paw, at day 1 after SNI surgery. ** p<0.05-WT ipsilateral hind paw vs. KO contralateral hind paw, at day 3 after SNI surgery. ** p<0.05-WT ipsilateral hind paw vs. KO contralateral hind paw, at day 7 after SNI surgery. * p<0.05- KO ipsilateral hind paw vs. KO contralateral hind paw, at 7 days after surgery. ** p<0.05-WT ipsilateral hind paw vs. KO contralateral hind paw, at day 14 after SNI surgery. * p<0.05- KO ipsilateral hind paw vs. KO contralateral hind paw, at 14 days after surgery. (WT n=4; KO n=6)*

With the purpose of assessing cold allodynia, the acetone test was performed on day -1, 1, 3, 7 and 14 of SNI. As depicted in Figure 24, all animals responded similarly before surgery (no response or fast hind paw removal considered as a 0.5 seconds time of response), indicating that cold allodynia was not present before the surgery and neuropathic pain development.

Unsurprisingly, one day after surgery, the injured hind paws of both animals (KO and WT) responded (lifted their paws) for a longer time to the acetone drop when compared with the corresponding uninjured hind paws (contralateral hind paw of WT and KO mice responded for 1.12±0.31s and 0.91±0.23s, respectively and ipsilateral hind paw responded for 3.50±1.04s in WT mice and for 2.66±0.61s in KO mice), confirming the development of cold allodynia. Though, only WT animals showed significant differences in their responses, comparing to the contralateral hind paw of KO animals ($p<0.05$, Figure 24). This significant response was also observed on day 7 after surgery.

On day 1 and 3 of SNI, there was a tendency for KO animals to have shorter duration responses, though there were no significant differences between genotypes, suggesting a tendency for KO mice to be more insensitive to cold stimuli. This is in agreement with previous results from our group indicating that chronic amylin administration aggravates cold allodynia in SNI-rats [75].

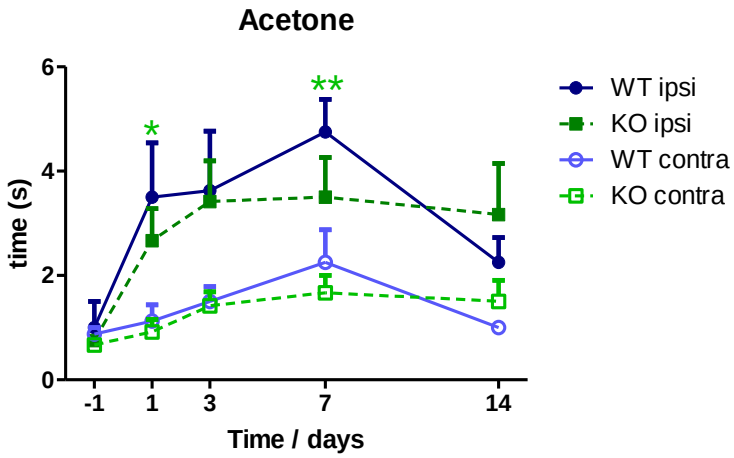

*Figure 24 - Assessment of cold allodynia by the acetone test, after SNI surgery in WT and KO mice. *p<0.05-WT ipsilateral hind paw vs. KO contralateral hind paw, at day 1 after SNI surgery. **p<0.01 WT ipsilateral hind paw vs. KO contralateral hind paw, 7 days after SNI surgery. (WT n=4; KO n=6)*

In the Hargreaves test, in which thermal hyperalgesia and allodynia were assessed, no significant differences were observed throughout most of the experimental period, except on day 7 after surgery, when WT animals exhibited a significantly lower PWL in their ipsilateral hind paw (4.58±0.46s), when comparing to both WT and KO contralateral hind paws (9.55±1.27s and 8.87±0.72s, respectively; $p<0.05$; Figure 25). At this time point of neuropathy, the ipsilateral PWL of KO animals did not show significant differences in comparison to all groups.

As expected, the PWL of ipsilateral hind paws of both groups of animals were lower than the values obtained in the contralateral control hind paws (Figure 25), which is a consequence of the SNI surgery.

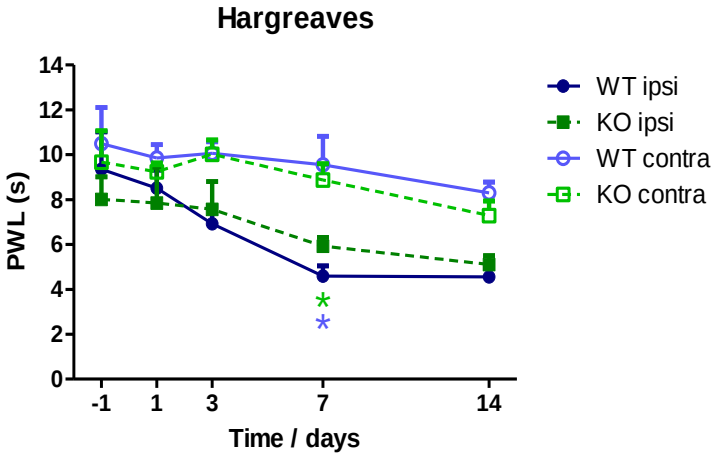

*Figure 25 - Thermal hyperalgesia and allodynia evolution in SNI pain model animals. *p<0.05- WT ipsilateral hind paw vs. WT contralateral hind paw, 7 days after SNI surgery. *p<0.05- WT ipsilateral hind paw vs. KO contralateral hind paw, 7 days after SNI surgery. (WT n=4; KO n=6)*

As aforementioned, the cold plate test was performed only at 14 days after surgery in order to assess cold hyperalgesia. The number of hind paw flinches was counted and the ipsilateral hind paw withdrawal latency was measured. As observed in Figure 26, the slight differences between the two genotypes were not statistically significant. There was a tendency for KO animals to flinch less often the affected hind paw (19.00±7.88 and 13.17±2.05 for WT and KO mice, respectively, Figure 26A) and to withdraw the same hind paw later in response to the stimulus (24.83±3.23 and 34.65±4.17 for WT and KO mice, respectively, Figure 26B). Both results are in accordance with each other, suggesting that KO SNI-animals tended to show greater tolerance to noxious cold than WT SNI-mice

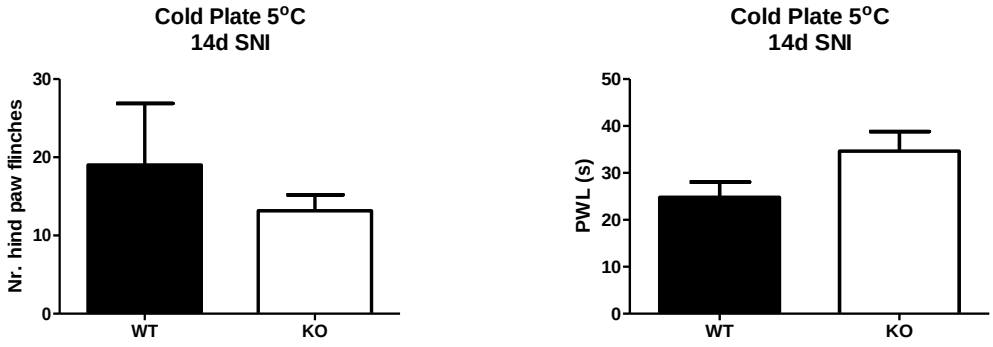

A B

Figure 26 - Cold Plate tests on KO (n=6) and WT (n=4) mice, 14 days after SNI pain model induction. A) number of ipsilateral hind paw flinches; B) ipsilateral hind paw withdrawal latency (PWL).

Taken together, these results suggest that the KO SNI-mice are less sensitive to the different applied stimuli, showing less signs of neuropathic pain. These results were supported by the expression of c-Fos, an immediate early gene that is rapidly and specifically expressed by spinal cord neurons in response to noxious stimulation [38].

Indeed, WT mice showed a significantly higher number of c-Fos positive neurons than KO mice (68.91±3.33 and 53.09±3.17 for WT and KO mice, respectively; $p<0.05$, Figure 27), suggesting that more spinal cord nociceptive-responsive neurons were activated in WT SNI-mice, which supports the results obtained in the behavioral tests. Thus, we can conclude that amylin KO mice displayed less pain-associated behaviors after SNI surgery than the WT animal group, suggesting that, in WT animals, amylin may play a role in the mechanisms leading to chronic pain settlement after peripheral nerve injury by promoting the development of allodynia and hyperalgesia.

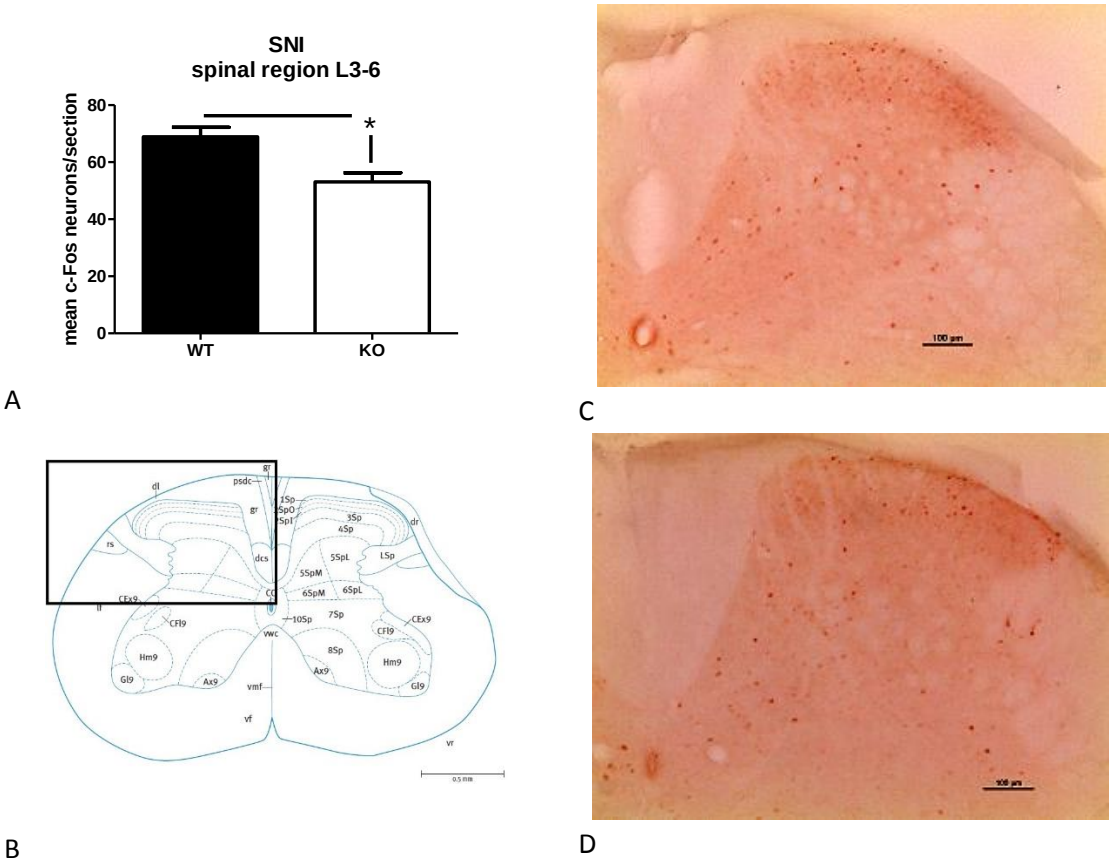

*Figure 27 - A) c-Fos quantification on the ipsilateral side of WT and KO animals' spinal cords, after 14 days of SNI surgery. *p<0.05- WT mice vs. KO mice; B) Schematic drawing of the L4 segment of the spinal cord (from [33]) representing the dorsal horn area used for c-Fos quantification; Microphotographs showing the c-Fos expression in ipsilateral site of L4 spinal cord slices. C) c-Fos immunohistochemistry in WT animal spinal cord; D) c-Fos immunohistochemistry in a KO animal spinal cord. WT n=4; KO n=5.*

Visceral pain model: The writhing test

After intraperitoneal injection of acetic acid, mice were placed in a plastic chamber and their behavior was video recorded for 20 minutes. Hyperalgesia was measured by counting the number of writhes in 5 minute time-periods for 20 minutes

(Figure 28A) and the total number of contractions between 5 and 15 minutes post-injection (Figure 28B), when pain behavior is usually maximal [24, 79].

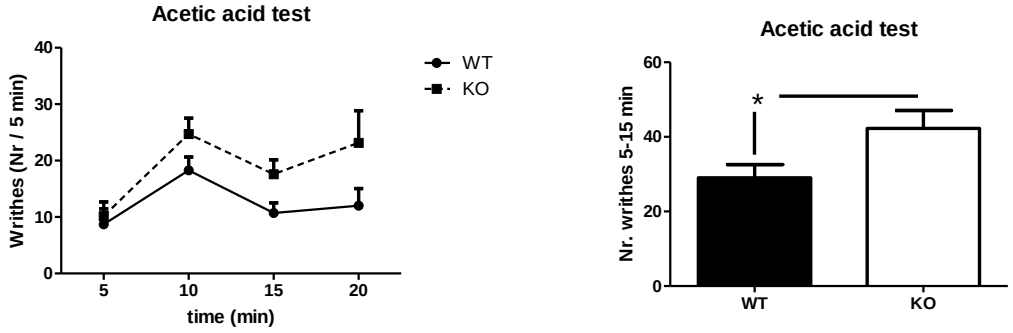

A *B*

Figure 28 - Writhing test in WT e KO mice after acetic acid injection. A) Number of writhes over 20 minutes. B) Total number of writhes after intraperitoneal injection of acetic acid, from 5 minutes after acetic acid injection to 15 minutes after acetic acid injection. p<0.05- WT mice vs. KO mice. WT n=7; KO n=7.*

As can be observed in Figure 28A, though there were no significant punctual differences between the two animal groups, there was a time effect, as KO and WT animals diverge over time (Figure 28A) with a tendency for amylin KO mice to display more writhes per 5 minutes at the later time points of the test (15 and 20 min). Accordingly, KO animals had in total significantly more writhes than WT animals, between minute 5 and minute 15 (29.00±3.57 and 42.29±4.76 for WT and KO mice, respectively; $p<0.05$, Figure 28B). Although there were no statistically significant differences for the number of writhes in 5 minute time-periods between genotypes (Figure 28A), this data is in agreement with data in Figure 28B, and altogether they suggest an anti-nociceptive role of amylin in visceral pain as amylin KO mice injected with acetic acid displayed more pain-related behaviors.

Moreover, the analysis of c-Fos expression after the writhing tests showed that KO mice expressed significantly more c-Fos than WT mice (Figure 29). This result is in agreement with the behavioral analysis, as more c-Fos expression is usually associated with more pain. These results comply with data from Huang et al (2000) that proposed an anti-nociceptive role of amylin as both intraperitoneal and intrathecal amylin administration attenuated the number of writhes in the same visceral pain model.

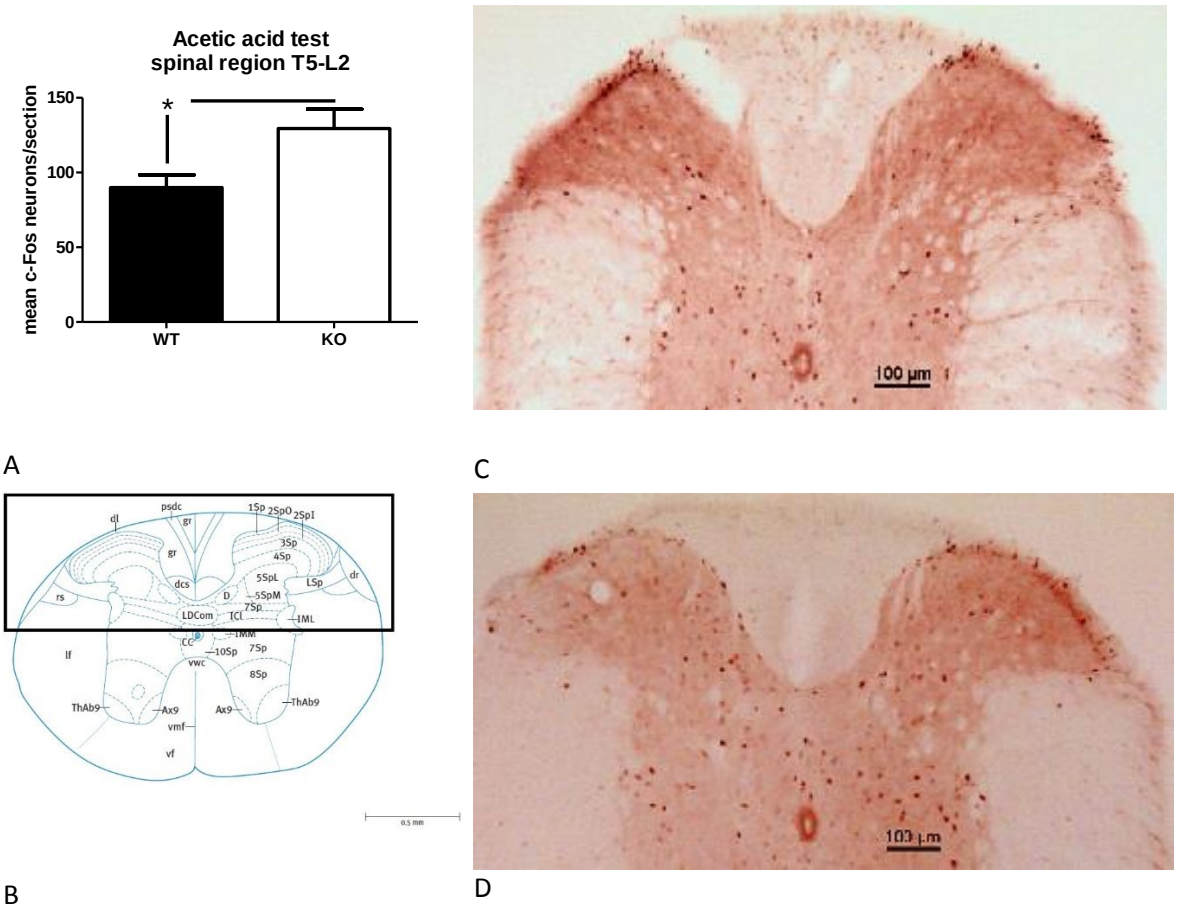

*Figure 29 - A) c-Fos quantification on WT and KO animals' spinal cords, after acetic acid injection. *p<0.05 B) Schematic drawing of the T13 segment of the spinal cord (from [33]) representing the dorsal horn area used for c-Fos quantification; Microphotographs showing the c-Fos expression in the dorsal horn of T13 spinal cord slices: C) c-Fos immunohistochemistry in WT animal spinal cord; D) c-Fos immunohistochemistry in KO animal spinal cord. WT n=6; KO n=6.*

Quantification of neuronal density and cell body area of DRG neurons

The hematoxylin and eosin (H&E) staining was performed to label all the cells in L4 and L5 DRG in naïve mice (Figure 30). This allowed inferring the neuronal density (Figure 30A) in the DRGs of both WT and KO mice groups, as well as the neuronal cell body areas and their categorization per size (Figure 30B).

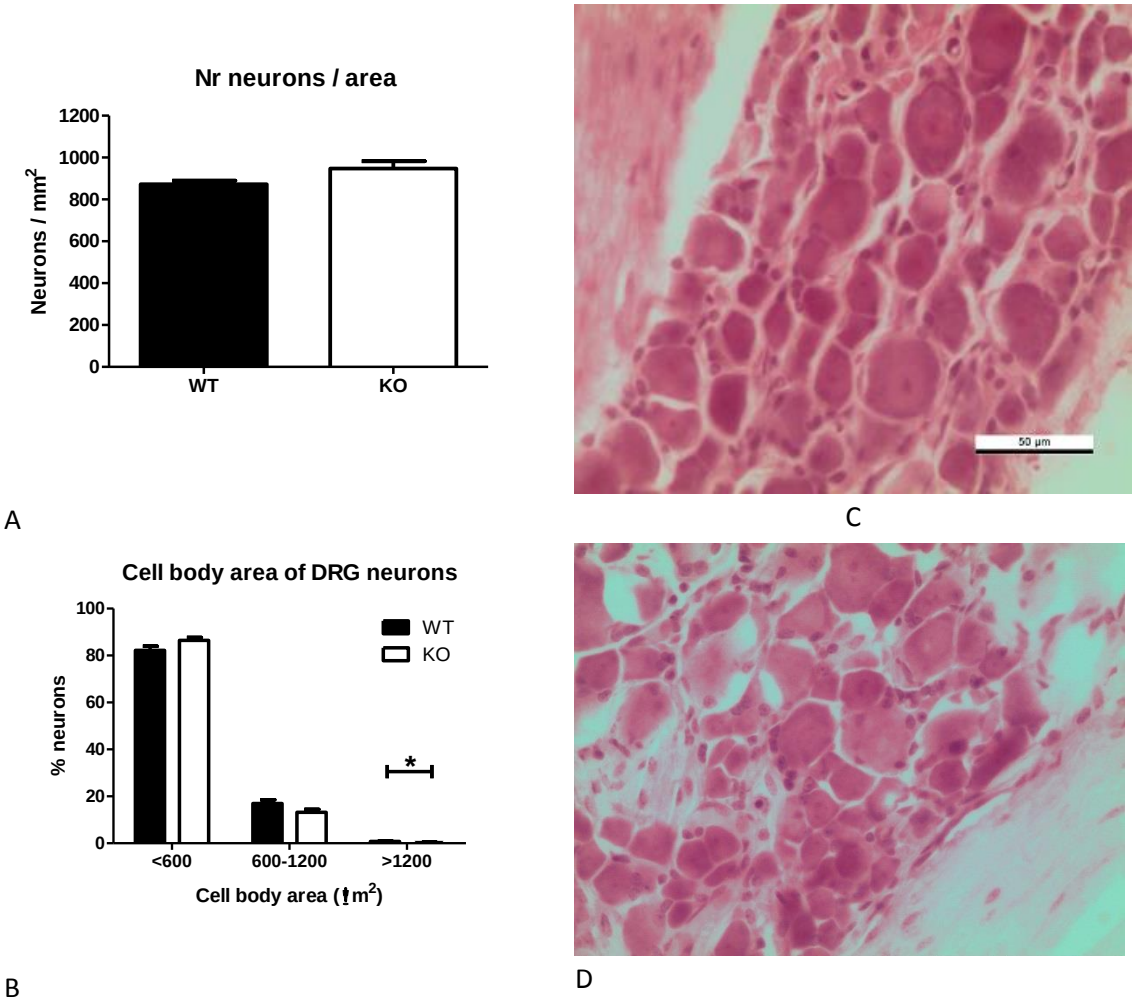

*Figure 30 - Neuronal density and cell body area in L4 and L5 DRGs from WT (n=4) and KO (n=5) naïve mice. A) Neuronal density in WT and KO naïve animals. B) Cell body areas distribution in WT and KO naïve mice. *p<0.05- cell body area>1200 WT vs. cell body area>1200 KO. C) Hematoxylin and eosin staining in a L5 DRG slice of WT mice. D) Hematoxylin and eosin staining in a L5 DRG section of KO mice*

As observed in Figure 30A, there were no significant variations on the neuronal density, when comparing WT and KO animals. Still, KO animals showed a slight increase in the number of neurons per area, although this was not significant, probably due to the low number of animals analyzed. This small trend can be explained by data regarding the average neuronal cell body area shown in Figure 30B). As shown, KO animals tended to have more small-sized neurons (<600 μm^2; 82.21±1.17 and 86.48±1.24 for WT and KO mice, respectively; p=0.08) and had significantly less large-sized neurons (>1200 μm^2), comparing to WT animals (0.82±0.16 and 0.32±0.10 for WT and KO mice, respectively; p<0.05).

In summary, in amylin KO mice, the large-sized neurons, known as Aβ, are scarce, while the small-sized neurons, presumably C and Aδ fibers, are in tendency more abundant. It has been reported that, in amylin KO mice, the number of neuronal cell bodies in DRGs was depleted until around birth [93]. Authors suggested a transitory role for amylin as a growth factor or a neurotrophic action in a subgroup of neurons that were replaced by other neuronal populations in the DRGs around birth.

The behavioral and histological results reported in this thesis support the latter possibility, in which amylin's lack leads to a misrepresentation of large-sized neurons and a compensatory tendency to a greater proportion of small-sized neurons in the DRGs. These small-sized neurons transmit noxious stimuli, which may in part explain the increased sensitivity observed by naïve amylin KO mice in acute mechanical pain tests.

The range of neuronal cell body areas obtained was similar to those previously described by similar studies [88, 94].

Immunohistochemistry results

Amylin immunolabeling

In order to confirm that KO animals did not express amylin in the nervous system, as expected since these animals have a generic ablation of the amylin gene in all body tissues, we performed an immunohistochemistry reaction for the detection of amylin's expression in the DRGs of both WT and KO mice groups (Figure 31). As shown, no amylin expression was found in KO mice DRG neurons, contrarily to WT mice in which many amylin-positive neurons could be observed.

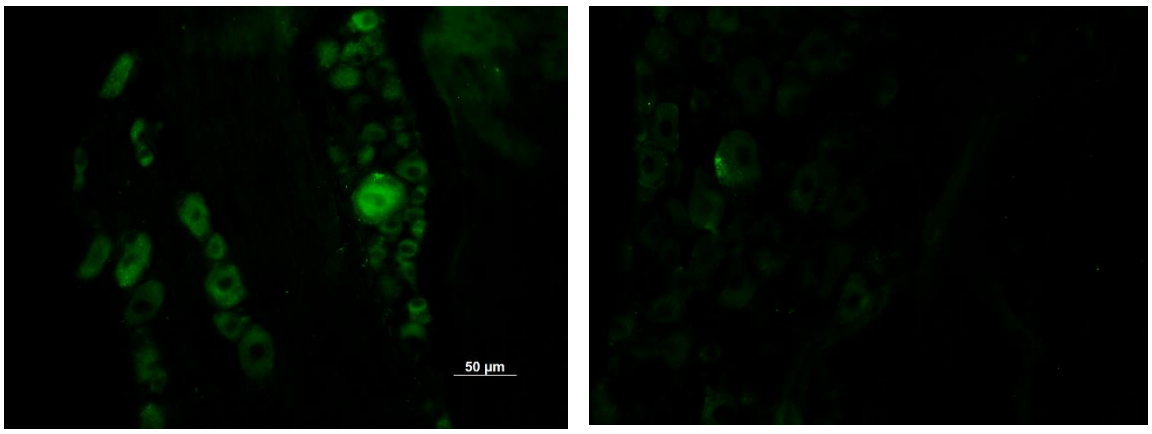

A B

Figure 31 - Fluorescence microphotographs of Immunohistochemistry reaction amylin (green) in lumbar 4 DRG of WT naïve mice (A) and KO naïve mice (B).

Quantification of CGRP expression

The percentage of neurons that expressed CGRP was quantified, as well as the areas of the same neurons, in order to assess whether behavioral changes in KO mice were caused by alterations in the number of C-peptidergic nociceptors or if CGRP would be expressed in amylin KO animals in a neuronal population with a size different

than what is normally observed in WT animals. As shown in Figure 32, there were no significant differences between WT and KO mice in the percentage of neurons which expressed CGRP in L4 and L5 DRGs (12.80±1.43 and 10.43±1.06 for WT and KO mice, respectively).

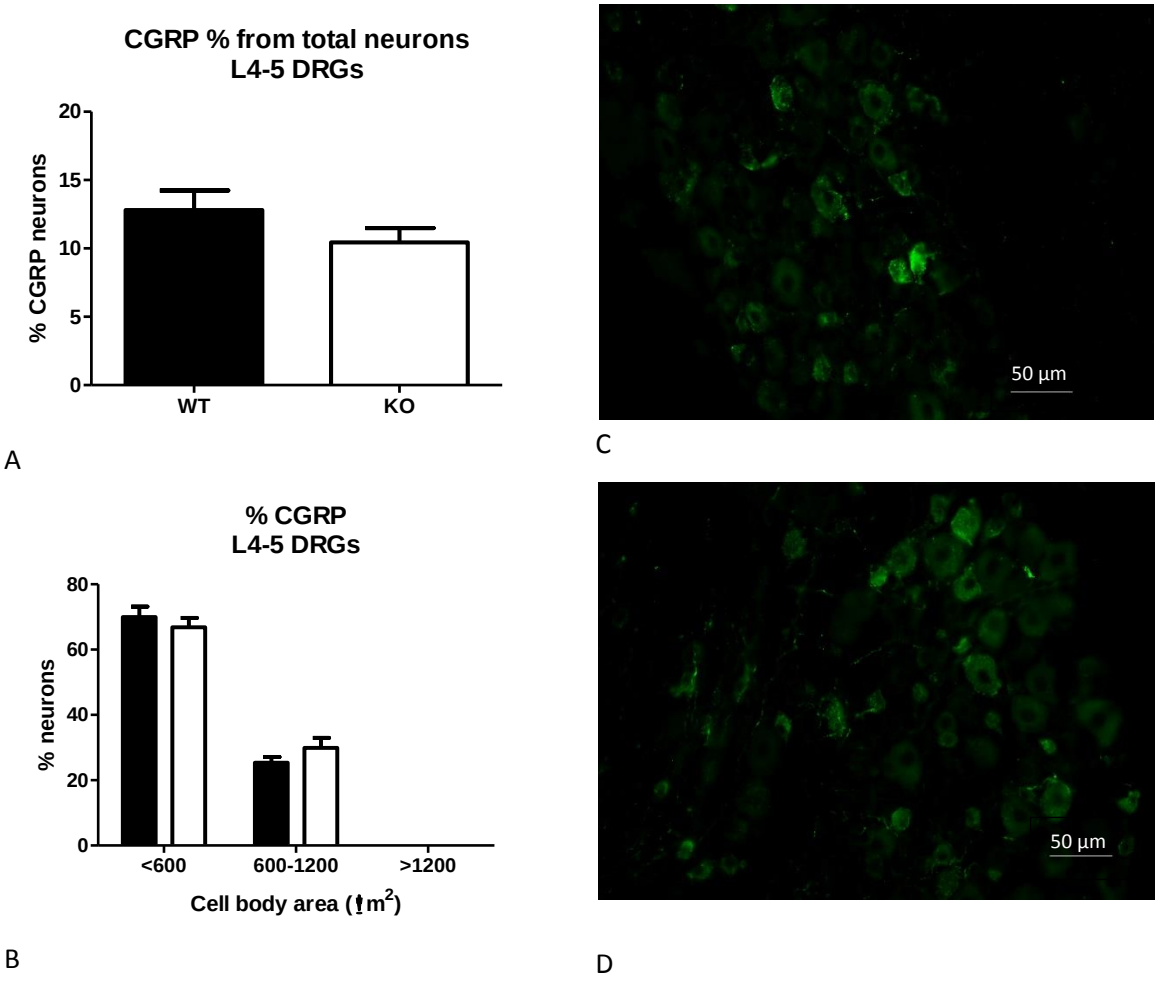

Figure 32 - Results from CGRP immunohistochemistry in lumbar 4 and 5 DRGs of WT (n=5) and KO (n=5) mice. A) Percentage of CGRP-positive neurons in L4 and L5 DRGs of WT and KO naive mice. B) cell area distribution of CGRP-positive neurons from L4 and L5 DRGs of WT and KO naive mice. Fluorescence microphotographs of lumbar 5 DRG in C) WT mice DRG after CGRP immunohistochemistry reaction. D) KO mice DRG after CGRP immunohistochemistry reaction

Additionally, KO animals have a tendency to have more medium-sized CGRP-positive neurons than WT mice (25.38±1.72 and 29.91±3.09 for WT and KO mice, respectively; Figure 32B). However, there were no significant differences on the area distribution of neurons expressing CGRP. Both animal groups had no CGRP-positive large-sized neurons, as expected.

Overall, we can say that KO mice did not reveal significant alterations in their C-peptidergic population of DRG neurons, proposing that the fibers which are related to the behavioral alterations in pain thresholds may be related to either C-non-peptidergic fibers or Aδ fibers. Still, this later possibility needs further study.

In summary, it is possible that the variations in KO mice pain behavior are not related with changes in C peptidergic fibers but may be caused by a phenotypic switch between neuronal types from Aβ to Aδ fibers, as amylin KO mice showed reduced numbers of large area neurons in the DRGs.

Conclusions and future perspectives

According to the acquired data, amylin's role in nociception seems to diverge depending on the pain model induced and on the nature of the noxious stimulus. In naïve mice, the results from both mechanical tests are in agreement and suggest that, in normal/basal conditions, amylin KO mice are generally more sensitive to mechanical stimuli than WT mice. Here, amylin displays a putative role as a neuropeptide promoting anti-nociception. Contrarily, when cold hyperalgesia was assessed by the cold plate test, amylin's role seemed to be pro-nociceptive, since WT animals were more sensitive to thermal stimulus. On the other hand, the Hargreaves test showed no significant differences between the two animals groups. These dissimilarities observed between the results of the two thermal types of stimuli lead us to believe that the channels which function as detectors of cold stimuli are altered in KO mice, since they respond to noxious cold in a different manner compared to WT animals. These channels, TRPM8, are expressed by A and C fibers. We hypothesize that the expression patterns of TRPM8 and/or that the A fibers on amylin KO mice may be altered. We considered no changes in C fibers, since they express the channels which function as detectors of heat stimulus (TRPV1), and we did not notice behavioral changes when heat stimuli were applied to both animal groups (WT and KO). Furthermore, there were no significant changes in the proportion of the CGRP neuronal population in the KO animals DRGs.

In the inflammatory pain model, induced by CFA, KO mice had higher response thresholds but significant differences between genotypes were not detected. However, as WT ipsilateral hind paws present significant differences comparing with the non-inflamed hind paws (WT and KO contralateral hind paws), contrarily to KO ipsilateral hind paws, we could conclude that WT mice were generally more responsive to the noxious stimuli applied, suggesting a pro-nociceptive role of amylin in this inflammatory pain model. The differences between genotypes could become more evident if we had increased the number of animals per experimental group, which would allow developing more solid conclusions on this pain model.

In the neuropathic pain model, induced by the spared nerve injury surgery, we could observe that amylin KO mice displayed less pain-associated behaviors after SNI surgery than the WT animal group, suggesting that, in WT animals, amylin may play a role in the mechanisms leading to chronic neuropathic pain settlement by promoting the development of allodynia and hyperalgesia.

The data from the visceral pain model suggest an anti-nociceptive role of amylin in visceral pain as amylin KO mice displayed more pain-related behaviors, contracting the abdomen more times. This is in line with reports of antinociceptive amylin effects in the same pain model, suggested to be mediated via the spinal cord, and further supports an endogenous role for this peptide in the modulation of visceral

pain. The c-Fos expression was also higher in the spinal cord of KO animals, supporting the behavioral tests results and suggesting that indeed larger amounts of noxious information reached the spinal cord in animals lacking amylin expression.

Taken together, the behavioral tests suggested different roles for amylin as a neuropeptide mediator in nociception, being anti-nociceptive in the visceral pain model and pro-nociceptive in the neuropathic and inflammatory pain models. In naïve mice, amylin displayed a pro-nociceptive role in the cold plate test (cold hyperalgesia) and an anti-nociceptive role in mechanical acute pain tests (mechanical allodynia and hyperalgesia).

Amylin KO mice have lower numbers of DRG neuronal cell bodies until around birth, suggesting that amylin might act as a growth or neurotropic factor for DRG neurons [93]. These amylin effects may influence pathways involved in pain processing, so its lack may lead to a misrepresentation of a subgroup of neurons or pathways and could therefore explain why adult amylin KO mice are deficient in aspects of nociception, as reported before for the formalin test model [2] and in the present manuscript. The neuronal quantification in the L4-5 DRGs of amylin KO mice and the determination of their cell body areas lead us to conclude that the large-sized neurons, known as Aβ, were scarce, while the small-sized neurons, presumably C and Aδ fibers, were in tendency more abundant. So, the Aβ neurons may be the neuronal population being affected during development in amylin KO mice. Small-sized neurons, which seem to be over-represented in amylin KO DRGs, are known to transmit noxious stimuli, which may in part explain the increased sensitivity observed by naïve amylin KO mice in acute mechanical pain tests. However, it is known that the somatosensory system suffers plastic changes under chronic pain conditions, so whether these changes are still observed in chronic pain animals is not known and needs to be investigated.

In order to understand amylin's role as a modulatory neuropeptide, it is essential to rescue the phenotype of the amylin KO mice by administering amylin while subjecting the animals to the same pain models. The construction of a conditional amylin KO mouse, in which the spatial and temporal expression of amylin may be controlled, will allow evaluating amylin's implication on the development of the somatosensory system.

The CGRP-positive neurons quantification revealed that KO mice did not display significant alterations in the C-peptidergic population of DRG neurons, suggesting that the variations in KO mice pain behavior are not due to C peptidergic fibers, but may be caused by a phenotypic switch between A-neuronal types, possibly from Aβ to Aδ fibers, as amylin KO mice showed reduced numbers of large area neurons in the DRGs. It has been reported that there is a phenotypic switching of CGRP expression in Aβ afferents following nerve injury, and that this is a fundamental mechanism for the

development of neuropathic tactile allodynia [95]. It would therefore be interesting to study whether CGRP expression would be altered in the SNI-model in amylin KO mice.

To conclude we can say that amylin displays different roles in nociception depending on the pain condition and on the nature of the stimulus induced. Additionally, we noticed an alteration in neuronal populations in the DRGs of KO mice. We also concluded that the variations in KO mice pain behavior are possibly not due to C peptidergic fibers but may be caused by a phenotypic switch between neuronal types from Aβ to Aδ fibers.

It is important to increase the number of animals per group of some experiments, in order to acquire more representative data regarding the groups' behavior and to allow a more solid statistical analysis. Moreover, it is essential to understand which specific fibers are affected by amylin, so we can clarify amylin's mechanisms and pathways involved in nociception. For that it will be important to perform additional immunohistochemical stainings of DRG sections with additional neuronal markers for A-fibers and C-non-peptidergic neurons.

References

1. Dickerson, I.M. *Receptors for the calcitonin family of neuropeptides*. 2015 [cited 2015 28-01-2015]; Available from: http://www.urmc.rochester.edu/labs/dickerson-lab/projects/.
2. Gebre-Medhin, S., et al., *Reduced nociceptive behavior in islet amyloid polypeptide (amylin) knockout mice.* Brain Res Mol Brain Res, 1998. **63**(1): p. 180-3.
3. Merskey, H. and F.G. Spear, *The concept of pain.* Journal of Psychosomatic Research, 1967. **11**(1): p. 59-67.
4. Castro-Lopes, J.M., *Fisiopatologia da dor*2003.
5. Zimmerman, M., *Physiological mechanisms of pain and its treatment.* Klinische Anaesthesiol Intensivether, 1986. **32**: p. 1-19.
6. Kafer, E., et al., *Biphasic depression of ventilatory response to C)2 following epidural morphine.* Anesthesiology, 1983. **58**: p. 418-427.
7. Bromage, P.R., *Epidural Narcotics for Postoperative Pain Relief.* Regional Anesthesia and Pain Medicine, 1982. **7**(4): p. 140-143.
8. Furlan, A.D., et al., *Opioids for chronic noncancer pain: a meta-analysis of effectiveness and side effects.* CMAJ : Canadian Medical Association Journal, 2006. **174**(11): p. 1589-1594.
9. Woolf, C.J., *What is this thing called pain?* J Clin Invest, 2010. **120**(11): p. 3742-4.
10. Millan, M.J., *The induction of pain: an integrative review.* Progress in Neurobiology, 1999. **57**(1): p. 1-164.
11. Muir, W.W., 3rd and C.J. Woolf, *Mechanisms of pain and their therapeutic implications.* J Am Vet Med Assoc, 2001. **219**(10): p. 1346-56.
12. Dubner, K.R.a.R., *Inflammatory Models of Pain and Hyperalgesia.* ILAR Journal, 1999. **40**.
13. Radhakrishnana R., Moorec S., and Sluka K., *Unilateral carrageenan injection into muscle or joint induces chronic bilateral hyperalgesia in rats.* International Association for the Study of Pain, 2003: p. 567–577.
14. Dubuisson, D. and S.G. Dennis, *The formalin test: A quantitative study of the analgesic effects of morphine, meperidine, and brain stem stimulation in rats and cats.* Pain, 1977. **4**(0): p. 161-174.
15. LaMotte, R.H., L.E. Lundberg, and H.E. Torebjörk, *Pain, hyperalgesia and activity in nociceptive C units in humans after intradermal injection of capsaicin.* The Journal of Physiology, 1992. **448**(1): p. 749-764.
16. Billiau, A. and P. Matthys, *Modes of action of Freund's adjuvants in experimental models of autoimmune diseases.* Journal of Leukocyte Biology, 2001. **70**(6): p. 849-860.
17. Snekhalatha, U., et al., *Evaluation of complete Freund's adjuvant-induced arthritis in a Wistar rat model.* Zeitschrift für Rheumatologie, 2013. **72**(4): p. 375-382.
18. Chillingworth, N.L. and L.F. Donaldson, *Characterisation of a Freund's complete adjuvant-induced model of chronic arthritis in mice.* Journal of Neuroscience Methods, 2003. **128**(1–2): p. 45-52.
19. Decosterd, I. and C.J. Woolf, *Spared nerve injury: an animal model of persistent peripheral neuropathic pain.* Pain, 2000. **87**(2): p. 149-158.
20. Ho Kim, S. and J. Mo Chung, *An experimental model for peripheral neuropathy produced by segmental spinal nerve ligation in the rat.* PAIN, 1992. **50**(3): p. 355-363.
21. Giamberardino, M.A., *Recent and forgotten aspects of visceral pain.* European Journal of Pain, 1999. **3**(2): p. 77-92.
22. Collier, H.O.J., et al., *THE ABDOMINAL CONSTRICTION RESPONSE AND ITS SUPPRESSION BY ANALGESIC DRUGS IN THE MOUSE.* British Journal of Pharmacology and Chemotherapy, 1968. **32**(2): p. 295-310.
23. Ness, T.J., *Models of Visceral Nociception.* ILAR Journal, 1999. **40**(3): p. 119-128.

24. Cho, I.-H., et al., *Minocycline markedly reduces acute visceral nociception via inhibiting neuronal ERK phosphorylation.* Molecular Pain, 2012. **8**(1): p. 1-13.
25. Fein, A., *Nociceptors and the perception of pain*2012, University of Connecticut Health Center.
26. Woolf, C.J. and Q. Ma, *Nociceptors—Noxious Stimulus Detectors.* Neuron, 2007. **55**(3): p. 353-364.
27. Caterina, M.J. and D. Julius, *Sense and specificity: a molecular identity for nociceptors.* Current Opinion in Neurobiology, 1999. **9**(5): p. 525-530.
28. Benarroch, E.E., *CGRP: sensory neuropeptide with multiple neurologic implications.* Neurology, 2011. **77**(3): p. 281-7.
29. Tredee R., et al., *Evidence for two different heat transduction mechanisms in nociceptive primary afferents innervating monkey skin*

Journal of Physiology, 1995. **483**.
30. Dubin, A.E. and A. Patapoutian, *Nociceptors: the sensors of the pain pathway.* The Journal of Clinical Investigation, 2010. **120**(11): p. 3760-3772.
31. Meyer, R.A., et al., *Mechanically insensitive afferents (MIAs) in cutaneous nerves of monkey.* Brain Research, 1991. **561**(2): p. 252-261.
32. Basbaum, A.I., et al., *Cellular and molecular mechanisms of pain.* Cell, 2009. **139**(2): p. 267-84.
33. Watson C., et al., *Atlas of the Mouse Spinal Cord*, in *The Spinal Cord: A Christopher and Dana Reeve Foundation Text and Atlas*, Watson C., Paxinos G., and K. G., Editors. 2009: London UK.
34. D'Mello, R. and A.H. Dickenson, *Spinal cord mechanisms of pain.* Br J Anaesth, 2008. **101**(1): p. 8-16.
35. Schmidtko, A., I. Tegeder, and G. Geisslinger, *No NO, no pain? The role of nitric oxide and cGMP in spinal pain processing.* Trends in Neurosciences. **32**(6): p. 339-346.
36. Hsieh, Y.-L., *Peripheral Therapeutic Ultrasound Stimulation Alters the Distribution of Spinal C-Fos Immunoreactivity Induced by Early Or Late Phase of Inflammation.* Ultrasound in Medicine and Biology. **34**(3): p. 475-486.
37. Hunt S., Pini A., and Evan G., *Induction of c-Fos-like protein in spinal cord neurons following sensory stimulation.* Nature, 1987. **328**.
38. Harris, J.A., *Using c-fos as a Neural Marker of Pain.* Brain Research Bulletin, 1998. **45**(1): p. 1-8.
39. Williams, S., G.I. Evan, and S.P. Hunt, *Changing patterns of c-fos induction in spinal neurons following thermal cutaneous stimulation in the rat.* Neuroscience, 1990. **36**(1): p. 73-81.
40. Abbadie, C. and J.M. Besson, *c-fos Expression in rat lumbar spinal cord during the development of adjuvant-induced arthritis.* Neuroscience, 1992. **48**(4): p. 985-993.
41. McCoy, E.S., B. Taylor-Blake, and M.J. Zylka, *CGRPα-Expressing Sensory Neurons Respond to Stimuli that Evoke Sensations of Pain and Itch.* PLoS ONE, 2012. **7**(5): p. e36355.
42. Reda, T.K., A. Geliebter, and F.X. Pi-Sunyer, *Amylin, Food Intake, and Obesity.* Obesity Research, 2002. **10**(10): p. 1087-1091.
43. Rojas, I. and A. Novials, *Amilina: del estudio molecular a las acciones fisiológicas*, in *Endocrinología y Nutrición*2001. p. 234-245.
44. Potes, C.S. and T.A. Lutz, *Brainstem mechanisms of amylin-induced anorexia.* Physiology & Behavior, 2010. **100**: p. 511-518.
45. Lutz, T.A., *Pancreatic Amylin as a Centrally Acting Satiating Hormone.* Current Drug Targets, 2005. **6**(2): p. 181-189.

46. Dégano, P., et al., *Amylin inhibits glucose-induced insulin secretion in a dose-dependent manner. Study in the perfused rat pancreas.* Regulatory Peptides, 1993. **43**(1–2): p. 91-96.
47. Hollander, P., et al., *Effect of Pramlintide on Weight in Overweight and Obese Insulin-Treated Type 2 Diabetes Patients.* Obesity Research, 2004. **12**(4): p. 661-668.
48. Harris, P.J., et al., *Amylin stimulates proximal tubular sodium transport and cell proliferation in the rat kidney*. Vol. 272. 1997. F13-F21.
49. Wookey, P., Z. Cao, and M. Cooper, *Interaction of the renal amylin and renin-angiotensin systems in animal models of diabetes and hypertension.* Mineral and electrolyte metabolism, 1999. **24**(6): p. 389-399.
50. Samonina, G.E., et al., *Antiulcer effects of amylin: a review.* Pathophysiology, 2004. **11**(1): p. 1-6.
51. Young, A.A., *Methods and compositions for treating pain with amylin or agonists thereof*, 1997, Google Patents.
52. Flood, J.F., et al., *Effects of amylin on appetite regulation and memory.* Canadian Journal of Physiology and Pharmacology, 1995. **73**(7): p. 1042-1046.
53. Clementi, G., et al., *Behavioral effects of amylin injected intracerebroventricularly in the rat.* Peptides, 1996. **17**(4): p. 589-591.
54. O'Halloran, D.J. and S.R. Bloom, *Calcitonin gene related peptide.* BMJ : British Medical Journal, 1991. **302**(6779): p. 739-740.
55. Lerner, U.H., *Deletions of genes encoding calcitonin/alpha-CGRP, amylin and calcitonin receptor have given new and unexpected insights into the function of calcitonin receptors and calcitonin receptor-like receptors in bone.* J Musculoskelet Neuronal Interact, 2006. **6**(1): p. 87-95.
56. Poyner, D.R., et al., *International Union of Pharmacology. XXXII. The mammalian calcitonin gene-related peptides, adrenomedullin, amylin, and calcitonin receptors.* Pharmacol Rev, 2002. **54**(2): p. 233-46.
57. Christopoulos, G., et al., *Multiple amylin receptors arise from receptor activity-modifying protein interaction with the calcitonin receptor gene product.* Mol Pharmacol, 1999. **56**(1): p. 235-42.
58. Tilakaratne, N., et al., *Amylin receptor phenotypes derived from human calcitonin receptor/RAMP coexpression exhibit pharmacological differences dependent on receptor isoform and host cell environment.* J Pharmacol Exp Ther, 2000. **294**(1): p. 61-72.
59. Pondel, M., *Calcitonin and calcitonin receptors: bone and beyond.* Int J Exp Pathol, 2000. **81**(6): p. 405-22.
60. Young, A., *Receptor Pharmacology*, in *Advances in Pharmacology*, Y. Andrew, Editor 2005, Academic Press. p. 47-65.
61. Sexton, P.M., et al., *In vitro autoradiographic localization of amylin binding sites in rat brain.* Neuroscience, 1994. **62**(2): p. 553-67.
62. Banks, W.A. and A.J. Kastin, *Differential permeability of the blood-brain barrier to two pancreatic peptides: insulin and amylin.* Peptides, 1998. **19**(5): p. 883-9.
63. Sibilia, V., et al., *Amylin compared with calcitonin: competitive binding studies in rat brain and antinociceptive activity.* Brain Res, 2000. **854**(1-2): p. 79-84.
64. Mulder, H., et al., *Islet amyloid polypeptide (amylin) is expressed in sensory neurons.* J Neurosci, 1995. **15**(11): p. 7625-32.
65. Mulder, H., et al., *Islet amyloid polypeptide and calcitonin gene-related peptide expression are upregulated in lumbar dorsal root ganglia after unilateral adjuvant-induced inflammation in the rat paw.* Brain Res Mol Brain Res, 1997. **50**(1-2): p. 127-35.

66. Mulder, H., et al., *Islet amyloid polypeptide and calcitonin gene-related peptide expression are down-regulated in dorsal root ganglia upon sciatic nerve transection.* Brain Res Mol Brain Res, 1997. **47**(1-2): p. 322-30.
67. Lutz, T.A., et al., *Amylin receptors mediate the anorectic action of salmon calcitonin (sCT).* Peptides, 2000. **21**(2): p. 233-238.
68. Szántó, J., et al., *Pain Killing with Calcitonin in Patients with Malignant Tumours.* Oncology, 1986. **43**(2): p. 69-72.
69. Szanto, J., N. Ady, and S. Jozsef, *Pain killing with calcitonin nasal spray in patients with malignant tumors.* Oncology, 1992. **49**(3): p. 180-2.
70. Armagan, O., et al., *Inhalation therapy of calcitonin relieves osteoarthritis of the knee.* J Korean Med Sci, 2012. **27**(11): p. 1405-10.
71. Candeletti, S. and S. Ferri, *Antinociceptive profile of intracerebroventricular salmon calcitonin and calcitonin gene-related peptide in the mouse formalin test.* Neuropeptides, 1990. **17**(2): p. 93-98.
72. Rosenfeld, M.G., et al., *Production of a novel neuropeptide encoded by the calcitonin gene via tissue-specific RNA processing.* Nature, 1983. **304**(5922): p. 129-135.
73. Bouali, S.M., S.J. Wimalawansa, and F.B. Jolicoeur, *In vivo central actions of rat amylin.* Regulatory Peptides, 1995. **56**(2–3): p. 167-174.
74. Potes, C.S., et al., *Amylin affects pain-related behaviors associated with the formalin test.* Neuroscience Meeting Planner, 2012.
75. Almeida, L.S.M.S.d., *Determinação do potencial efeito anti- ou pro-nociceptivo da amilina num modelo animal de dor neuropática*, in *Departamento de Quimica e Bioquimica*2013, Faculdade de Ciências da Unicersidade do Porto Porto. p. 94.
76. Caria, J.P.F.d., *Efeito da amilina num modelo animal de dor crónica inflamatória*, 2012, Faculdade de Medicina da Universidade do Porto.
77. Zimmerman, M., *Ethical guidelines for investigations of experimental pain in conscious animals.* Pain, 1983. **16**: p. 109-110.
78. Ottoni, E.B., *EthoLog 2.2: a tool for the transcription and timing of behavior observation sessions. Behav Res Methods Instrum Comput 32* 2000.
79. Huang, X., et al., *Amylin suppresses acetic acid-induced visceral pain and spinal c-fos expression in the mouse.* Neuroscience, 2010. **165**(4): p. 1429.
80. Butler, S.H., et al., *A limited arthritic model for chronic pain studies in the rat.* Pain, 1992. **48**(1): p. 73-81.
81. Castro-Lopes JM, et al., *Increase in GABAergic Cells and GABA Levels in the Spinal Cord in Unilateral Inflammation of the Hindlimb in the Rat.* European Journal Neuroscience, 1992. **4**: p. 296-301.
82. Richner, M., et al., *The Spared Nerve Injury (SNI) Model of Induced Mechanical Allodynia in Mice.* 2011(54): p. e3092.
83. Tal M and B. GJ., *Extra-territorial pain in rats with a peripheral mononeuropathy: mechano-hyperalgesia and mechano-allodynia in the territory of an uninjured nerve.* Pain, 1994. **57**: p. 375-82.
84. Elhabazi, K., et al., *Assessment of morphine-induced hyperalgesia and analgesic tolerance in mice using thermal and mechanical nociceptive modalities.* J Vis Exp, 2014(89): p. e51264.
85. Allchorne, A.J., D.C. Broom, and C.J. Woolf, *Detection of cold pain, cold allodynia and cold hyperalgesia in freely behaving rats.* Molecular Pain, 2005. **1**: p. 36-36.
86. Hargreaves, K., et al., *A new and sensitive method for measuring thermal nociception in cutaneous hyperalgesia.* Pain, 1988. **32**(1): p. 77-88.
87. Yoon, C., et al., *Behavioral signs of ongoing pain and cold allodynia in a rat model of neuropathic pain.* Pain, 1994. **59**(3): p. 369-376.

88. Negri, L., et al., *Impaired Nociception and Inflammatory Pain Sensation in Mice Lacking the Prokineticin Receptor PKR1: Focus on Interaction between PKR1 and the Capsaicin Receptor TRPV1 in Pain Behavior.* The Journal of Neuroscience, 2006. **26**(25): p. 6716-6727.
89. Xu, Y., et al., *Ontogeny of Excitatory Spinal Neurons Processing Distinct Somatic Sensory Modalities.* The Journal of Neuroscience, 2013. **33**(37): p. 14738-14748.
90. Kobayashi, K., et al., *Distinct expression of TRPM8, TRPA1, and TRPV1 mRNAs in rat primary afferent neurons with adelta/c-fibers and colocalization with trk receptors.* J Comp Neurol, 2005. **493**(4): p. 596-606.
91. Mulder, H., et al., *Islet amyloid polypeptide and calcitonin gene-related peptide expression are upregulated in lumbar dorsal root ganglia after unilateral adjuvant-induced inflammation in the rat paw.* Molecular Brain Research, 1997. **50**(1–2): p. 127-135.
92. Bourquin, A.F., et al., *Assessment and analysis of mechanical allodynia-like behavior induced by spared nerve injury (SNI) in the mouse.* Pain, 2006. **122**(1-2): p. 14 e1-14.
93. Wookey, P.J., T.A. Lutz, and S. Andrikopoulos, *Amylin in the periphery II: An updated mini-review.* ScientificWorldJournal, 2006. **6**: p. 1642-55.
94. Pradier, B., et al., *Smad-interacting protein 1 affects acute and tonic, but not chronic pain.* Eur J Pain, 2014. **18**(2): p. 249-57.
95. Nitzan-Luques, A., et al., *Dynamic genotype-selective "phenotypic switching" of CGRP expression contributes to differential neuropathic pain phenotype.* Exp Neurol, 2013. **250**: p. 194-204.

Annexes

Genotyping protocol of mice IAPP

For the DNA extraction:

1. Prepare fresh NaOH solution by adding a NaOH pellet in 50mL of H_2O milliQ
2. Add 600uL NaOH solution to each tube
3. Piercing the eppendorf containing mouse tissue fragment
4. Put at 99 °C for 10min to 1h
5. Allow to cool
6. Add 100uL 1M Tris-HCl pH 8.0.

For the PCR reaction (20uL in each tube):

1. H_2O 10.9 µL
2. Taq polimerase Citomed 0.1 µL
3. Buffer 10x 2 µL
4. MgSO4 2 µL
5. Primer 206 10uM 1 µL
6. Primer 207 10uM 1 µL
7. Primer 208 10uM 1 µL
8. Primer 209 10uM 1 µL
9. Sample DNA 1 µL

Reactions condition:

95°C	5	min	
95°C	30	sec	35 cycles
62°C	30	sec	
72°C	30	sec	
72°C	10	min	

Electrophoresis in agarose 2% gel

Results:

- wild-type allele 100bps
- mutated allele 200bps

Complete Freund's Adjuvant

In a 50 mL flask place 60 mg of *Mycobacterium butyricum* and then add (drop by drop with agitation):

1. 6 mL paraffin oil;
2. 4 mL NaCl 0,9%;
3. 1 mL Tween 80;
4. 2.75 mg of azide.

Autoclave the flask at 121 ºC for 20 minutes. Allow it to cool and place at 4ºC.

Cryoprotector (1000mL):

a) 0.4M PBS pH 7.2 - 125mL;

b) Saccharose (Merck, Darmstadt) – 330 g;

c) Ethylene glycol (Merck, Darmstadt) - 300 mL;

d) Make up the volume to 1000 mL with distilled water.

Hydrogen Peroxide 1% (at 1% H2O2):

a) H_2O_2 30% (Merck, Darmstadt) - 330µL;

b) PBS - 10 mL.

Normal swine serum (NSS, Normal English Suine Serum) 2% in PBS / T 0.1M (50mL):

a) 1 mL of NSS;

b) Make up to 50 ml with PBS / T 0.1M.

Phosphate buffer (PB) to 0.4M - stock solution (2500mL):

a) 26.2g of hydrated sodium dihydrogen phosphate ($NaH_2PO_4.H_2O$; Merck, Darmstadt);

b) 140g of potassium phosphate (K_2HPO_4; Merck, Darmstadt);

c) Dilute a total volume of 2500mL of distilled water;

d) Check pH (7.2-7.4).

Phosphate Buffered Saline (PBS) 0.1M (1000mL):

a) Phosphate Buffer - 250 mL;

b) Distilled water - 750 mL;

c) NaCl (Merck, Darmstadt) - 9 g.

Phosphate Buffer Saline with Triton X-100 (PBS / T) 0.1M (1000mL):

a) Phosphate Buffer - 250 mL;

b) 3 mL of Triton X-100 or 12 mL solution of 25% Triton X.100;

c) NaCl - 9 g;

d) Make up the volume to 1000 mL with distilled water.

0.1M Tris-HCl buffer, pH 7.6:

a) 0.2M Tris (Merck, Darmstadt) – 12.1g in 500 mL of distilled water;

b) 1N HCl (Merck, Darmstadt) – 8.3mL in 100 mL of distilled water.